Antelope Structural Health Monitoring Applications

Frank Vernon
Virtual Antelope User Group
19 January 2023

UC San Diego | SCRIPPS INSTITUTION OF OCEANOGRAPHY

Overview

- 2017 Large High-Performance Outdoor Shake Table (LHPOST)
- 2021 Geisel Library Monitoring
- 2022 Six Degree-of-Freedom Upgrade to LHPOST6

1-DOF Large High-Performance Outdoor Shake Table (LHPOST) 2004-2019

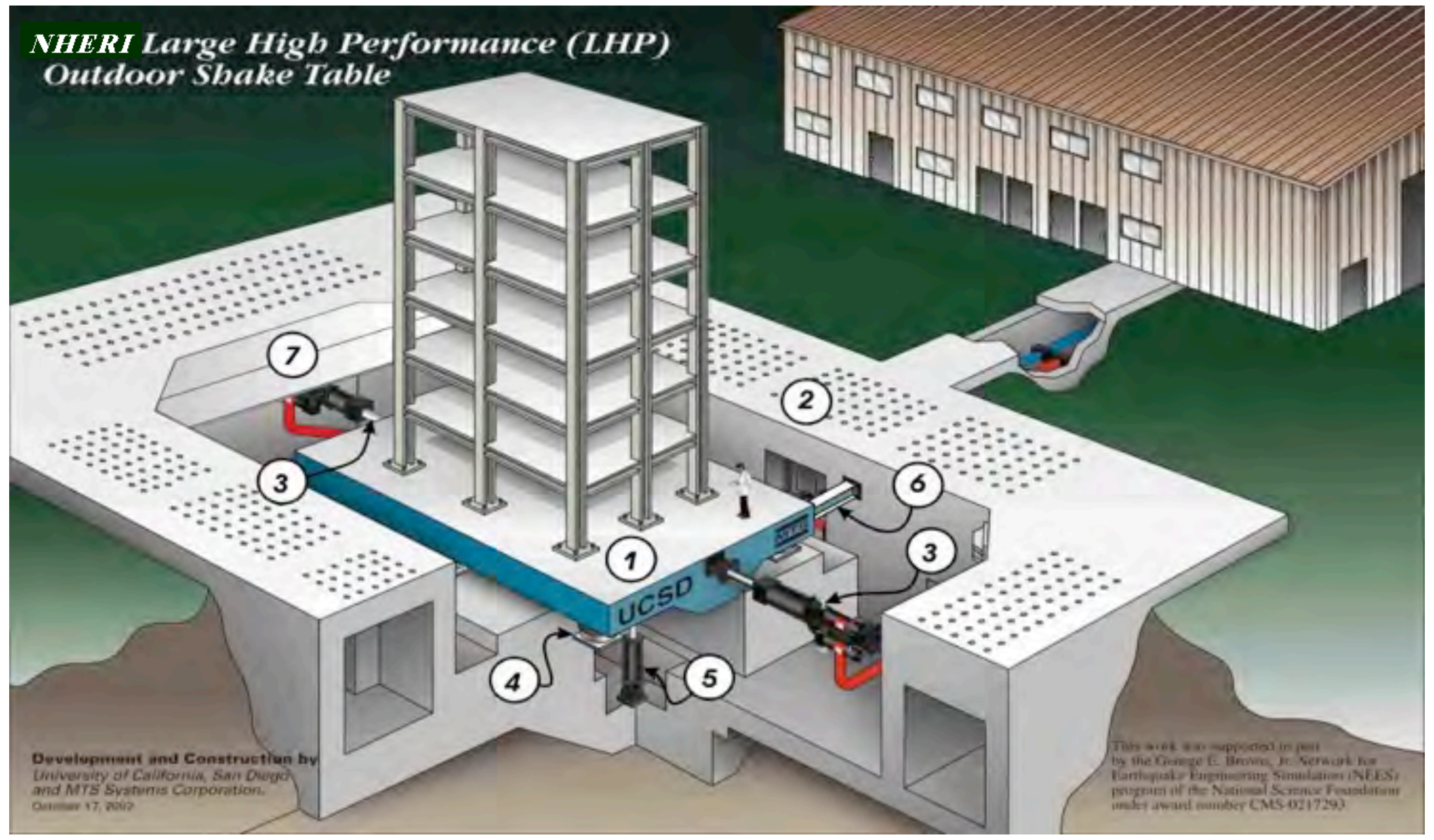

Performance Characteristics of LHPOST in Past 1-DOF Configuration (2004 – 2019)	
Designed as a 6-DOF shake table, but built as a 1-DOF system to meet funding available	
Stroke	**±0.75m**
Platen Size	40 ft × 25 ft (12.2 m × 7.6 m)
Peak Velocity	**1.8 m/sec**
Peak Acceleration	4.7g (bare table condition); 1.2g (4.0MN/400 tonf rigid)
Frequency Bandwidth	**0-33 Hz**
Horizontal Actuators Force	**6.8 MN (680 tonf)**
Vertical Payload Capacity	**20 MN (2,000 tonf)**
Overturning Moment Capacity	50 MN-m (5,000 tonf-m)

UCSD LHPOST 2017

- Largest shake table in US
- Development and Validation of a Resilience-based Seismic Design Methodology for Tall Wood Buildings: Phase I Test
- demands for tall residential and mixed-use buildings in the range of 8~20 stories are increasing.
- One new structural system in this height range are tall wood buildings which have been built in select locations around the world using a relatively new heavy timber structural material known as cross laminated timber (CLT).
- The majority of existing tall CLT buildings are located in non-seismic or low-seismic regions of the world.

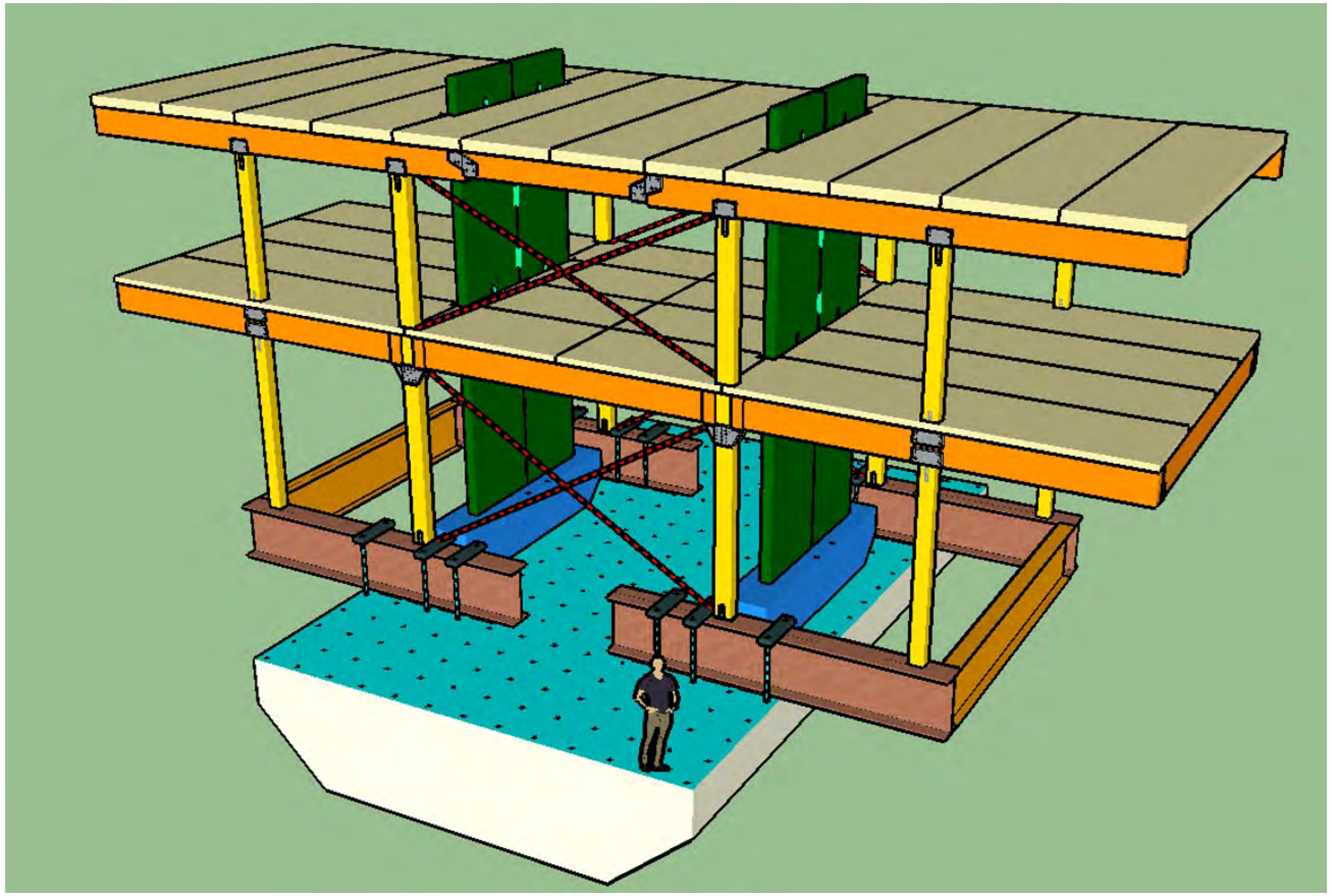

UCSD LHPOST 2017

- Largest shake table in US
- Development and Validation of a Resilience-based Seismic Design Methodology for Tall Wood Buildings: Phase I Test
- demands for tall residential and mixed-use buildings in the range of 8~20 stories are increasing.
- One new structural system in this height range are tall wood buildings which have been built in select locations around the world using a relatively new heavy timber structural material known as cross laminated timber (CLT).
- The majority of existing tall CLT buildings are located in non-seismic or low-seismic regions of the world.

Northridge - Max Credible Eq * 1.2

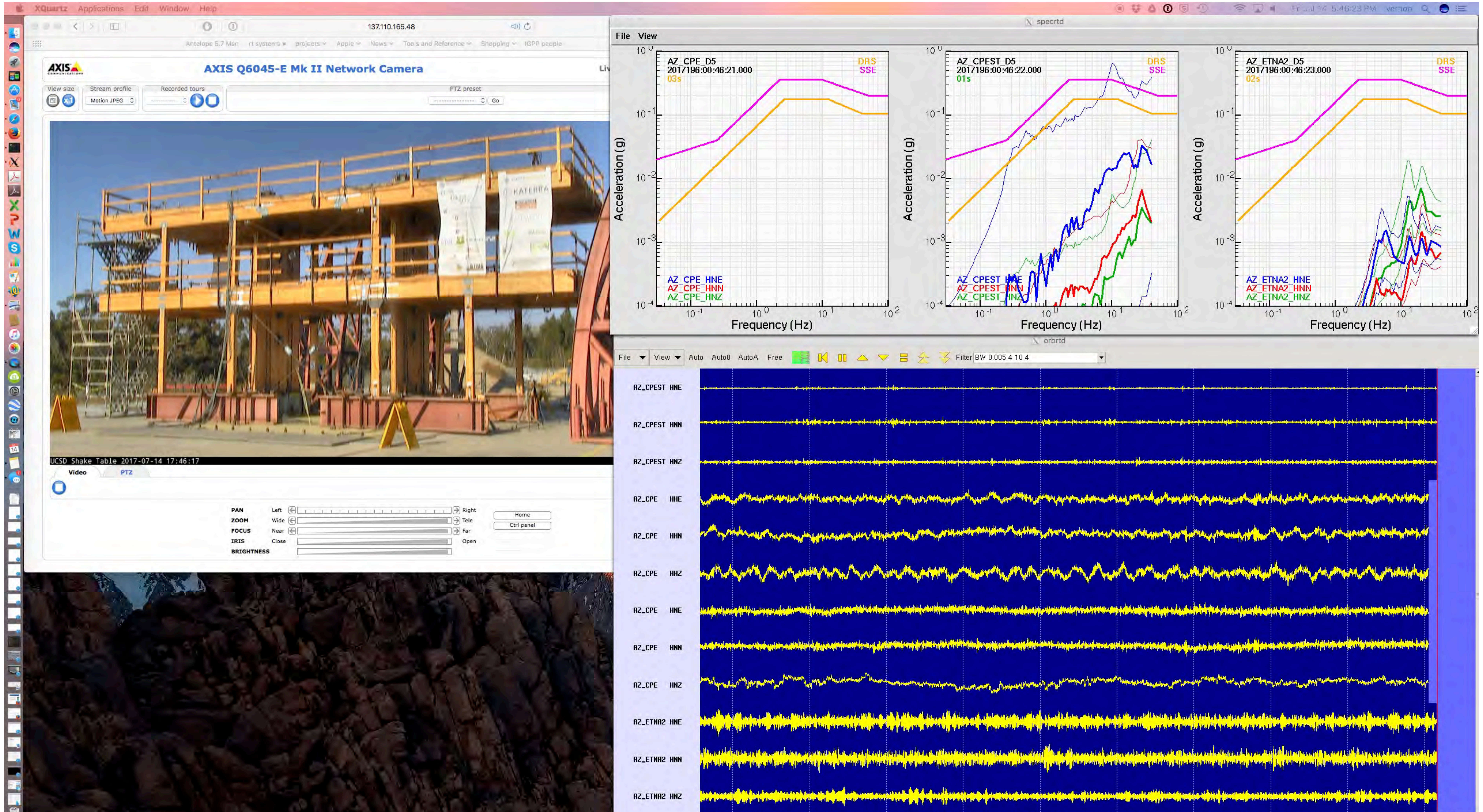

Geisel Library, UC San Diego

- Designed by William Pereira and opened in 1970 as the Central Library.
- 8-story (5 above ground and two underground)
- Landmark and iconic building of brutalist architecture, built in 1968.
- Renamed in 1995 in honor of Audrey and Theodor Seuss Geisel.

Geisel Library and Instrumentation

UC San Diego Collaborators

Lin Sun
Joel Conte
Michael Todd
Yehuda Bock
Glen Offield
Frank Vernon

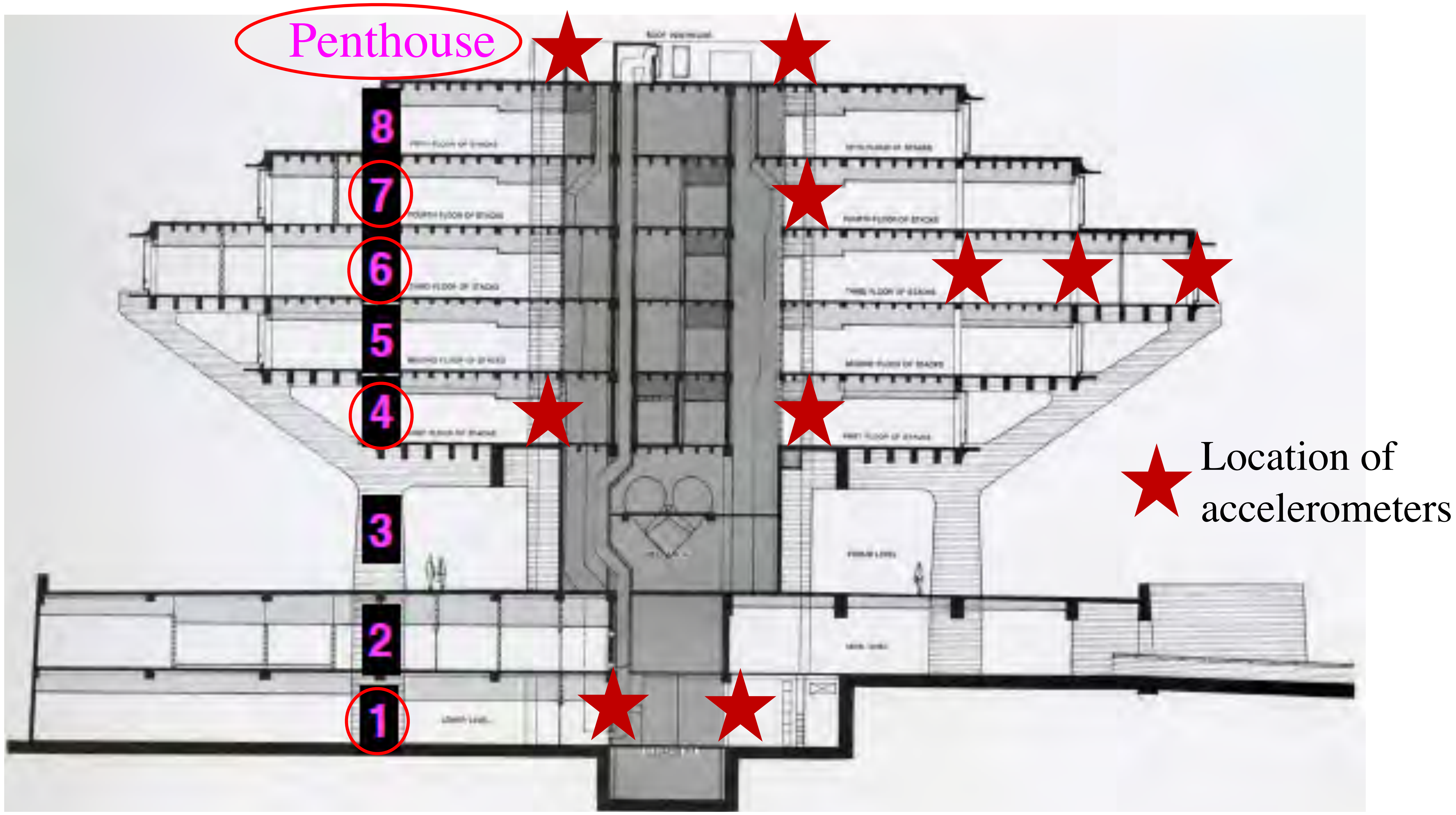

Elevation View of the Geisel Library and Instrumentation Plan

Geisel Library and Instrumentation

Top View of Library Rooftop

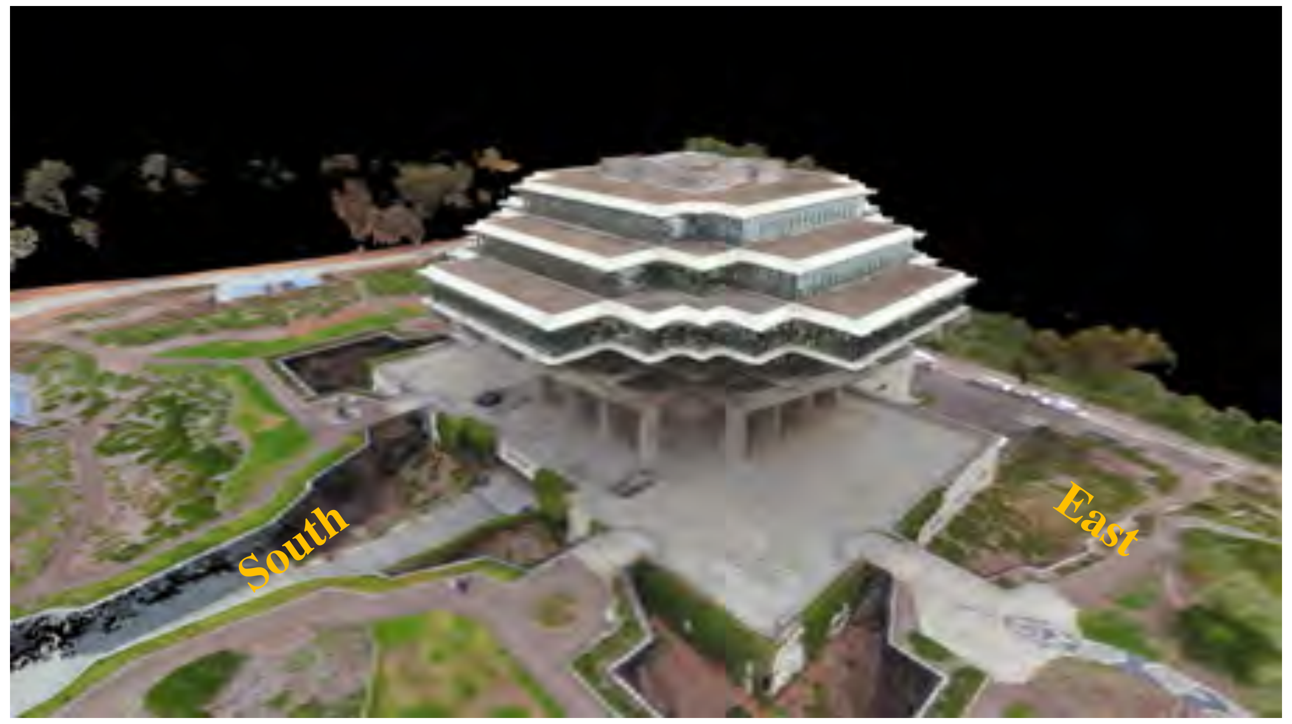

Perspective View of Library

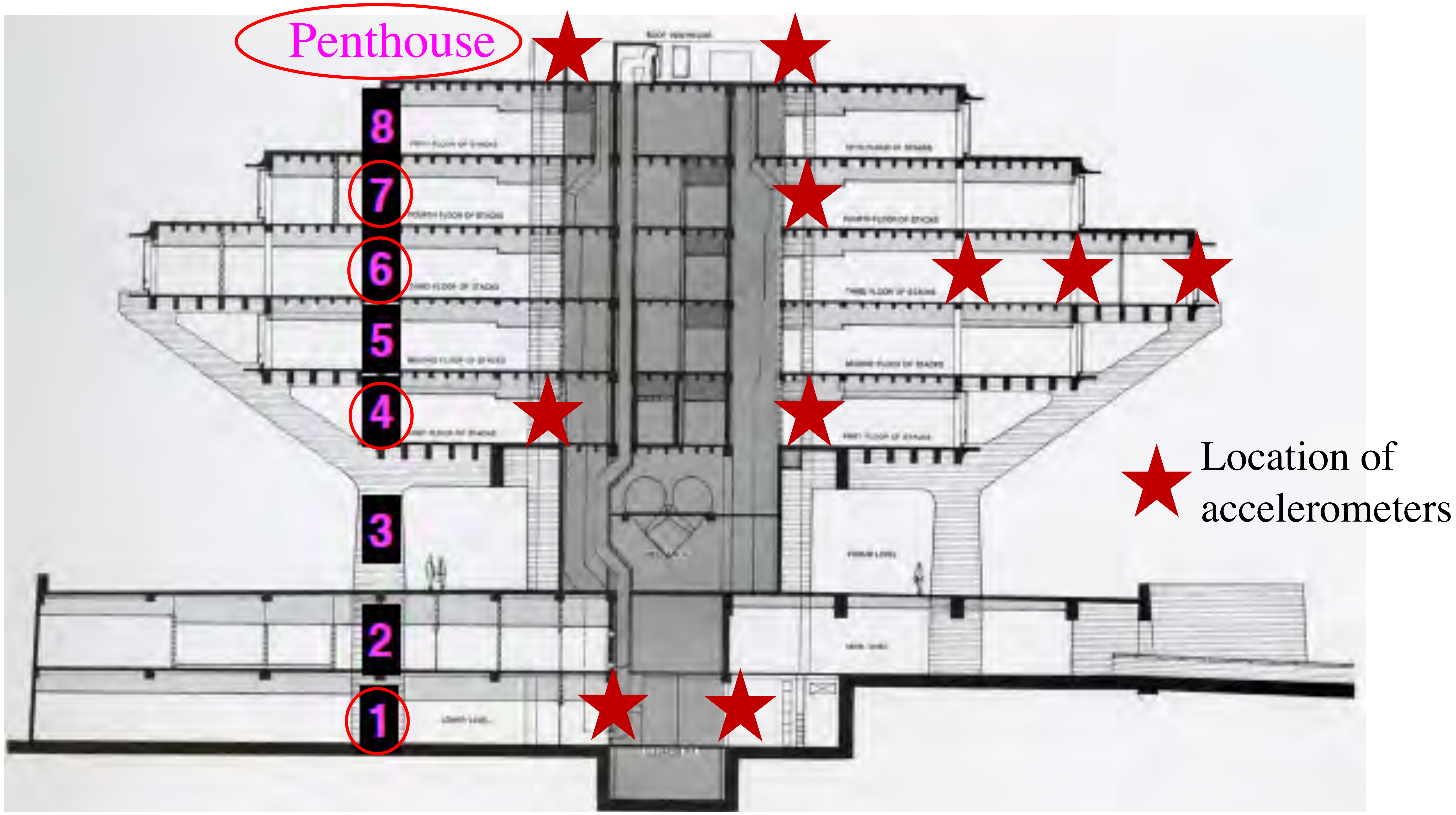

Elevation View of the Geisel Library and Instrumentation Plan

Geisel Library and Instrumentation

System Design

Antelope Real Time Data Acquisition
- Synchronous sampling
- Continuous (gapless) data
- Long term monitoring

Kinematrics Etna2 accelerometers
- Sampling rate: 200 Hz
- ± 2g span

Vaisala WXT536 Meteorological sensor
- Sampling rate: 0.1 Hz
- temperature
- atmospheric pressure
- relative humidity
- wind speed and direction
- rainfall

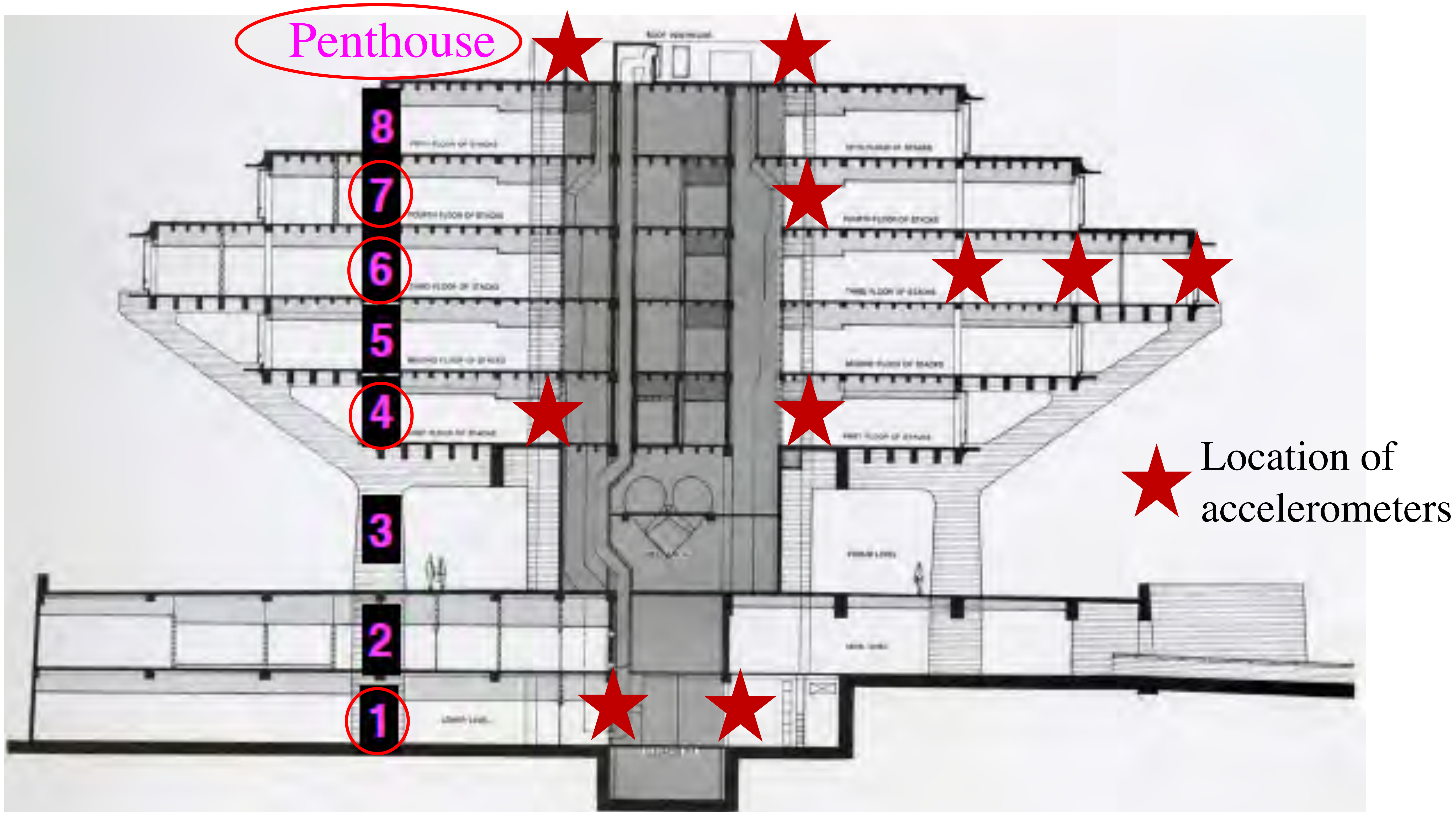

Elevation View of the Geisel Library and Instrumentation Plan

Locations of Accelerometers at Different Floors

Etna2 Accelerometer

First floor

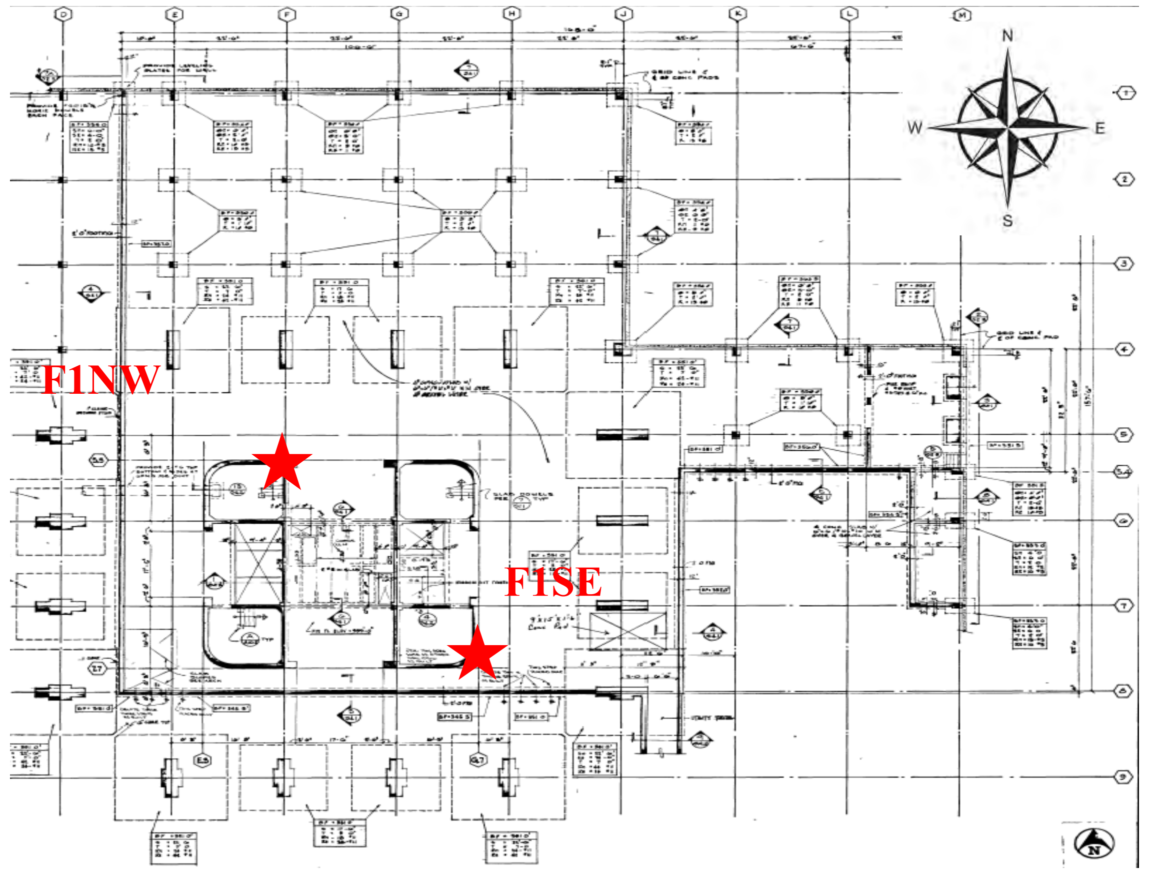

Fourth floor

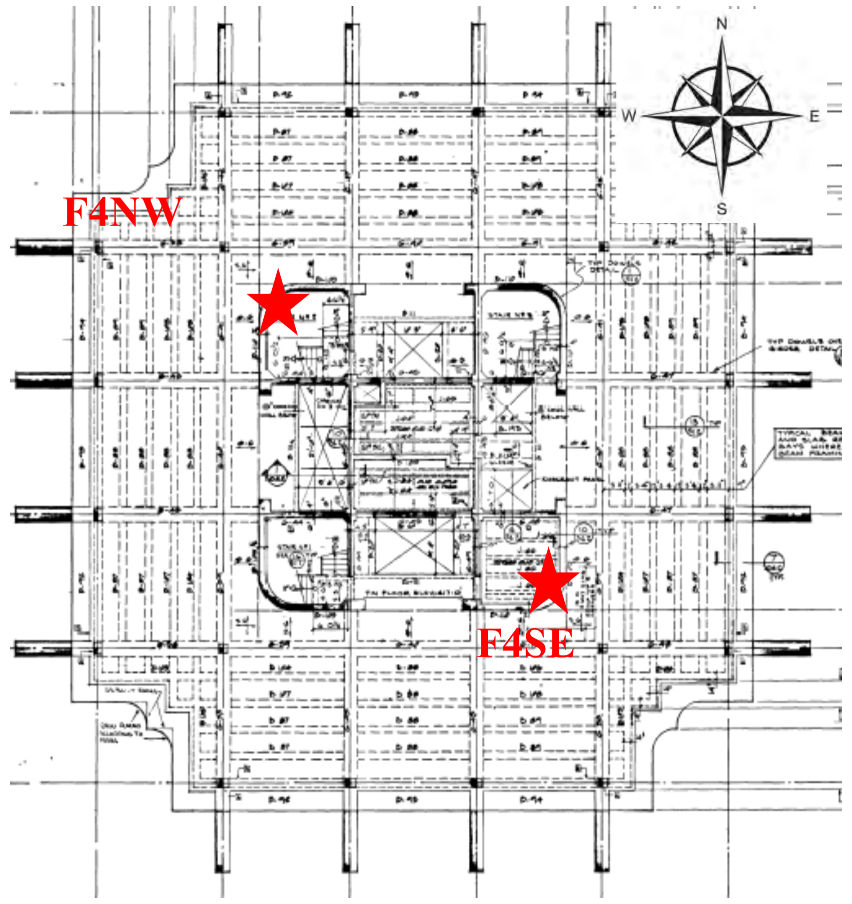

Sixth floor

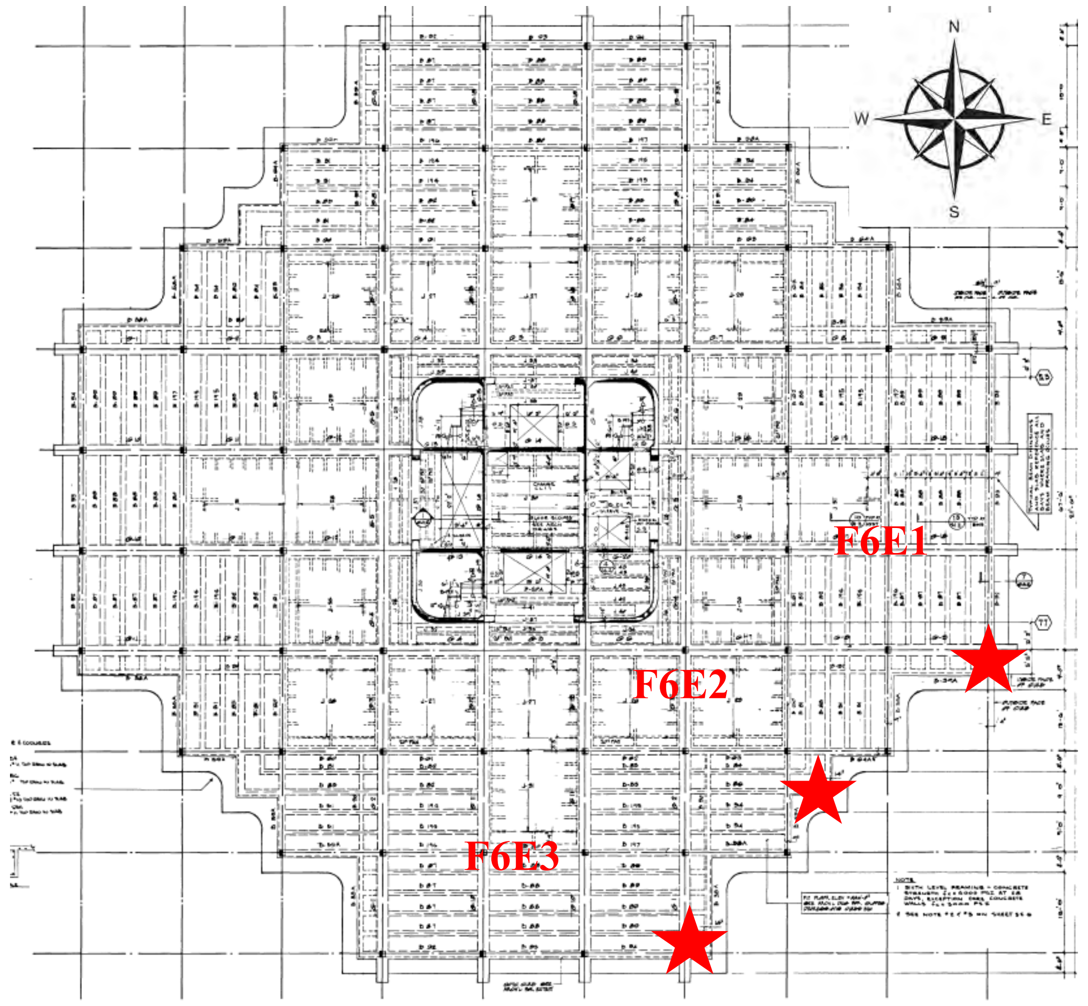

Seventh floor

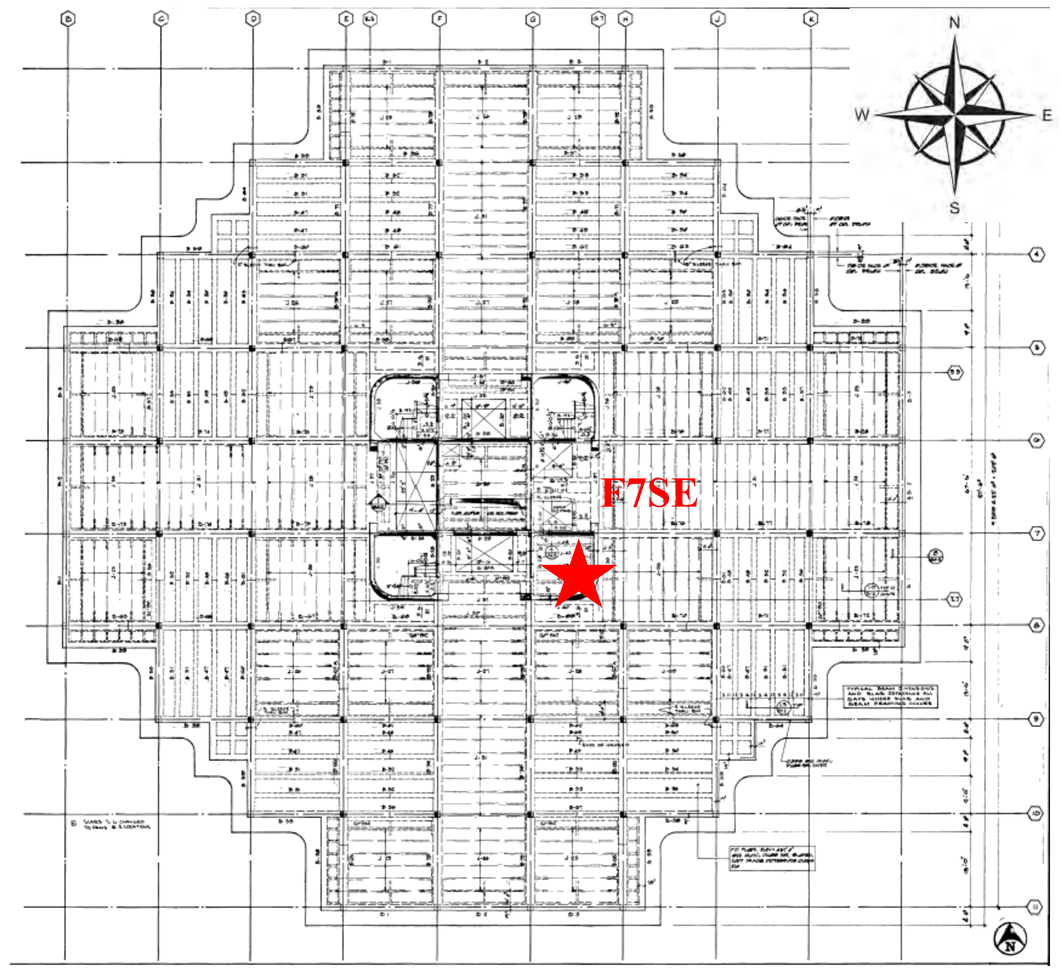

Roof (Penthouse)

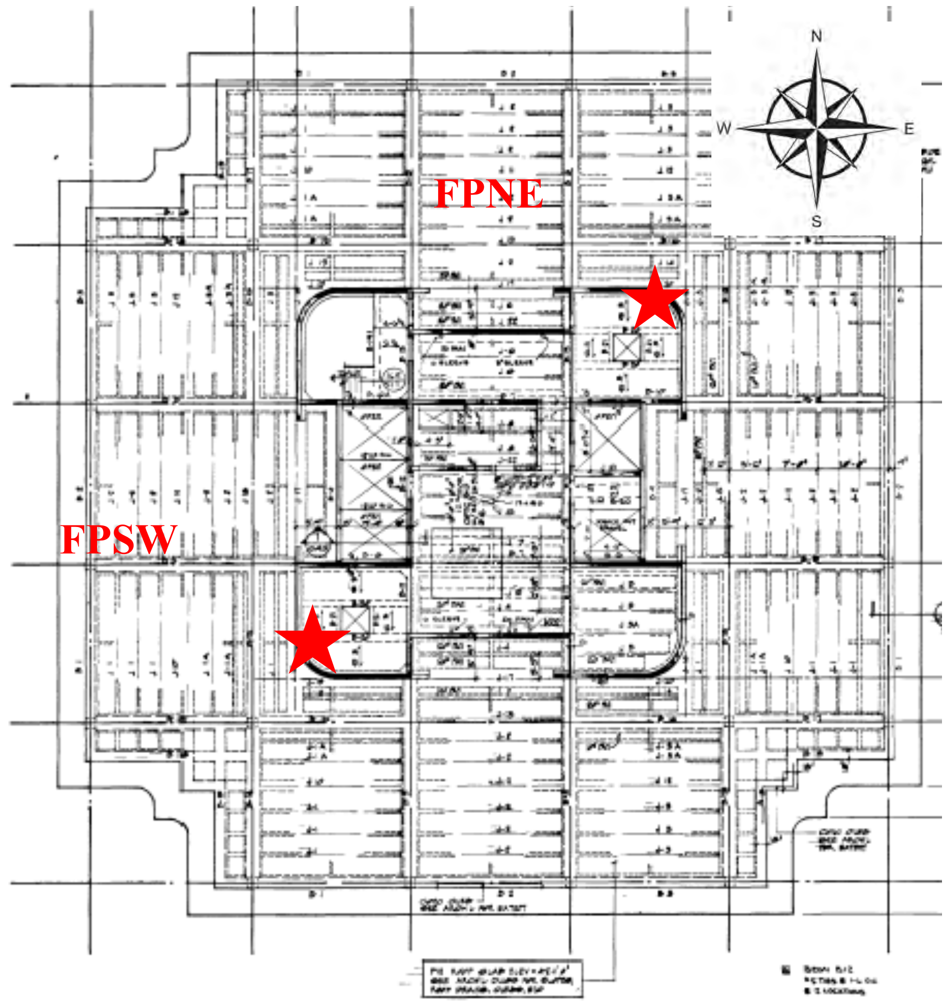

Locations of Accelerometers at Different Floors

Etna2 Accelerometer

First floor

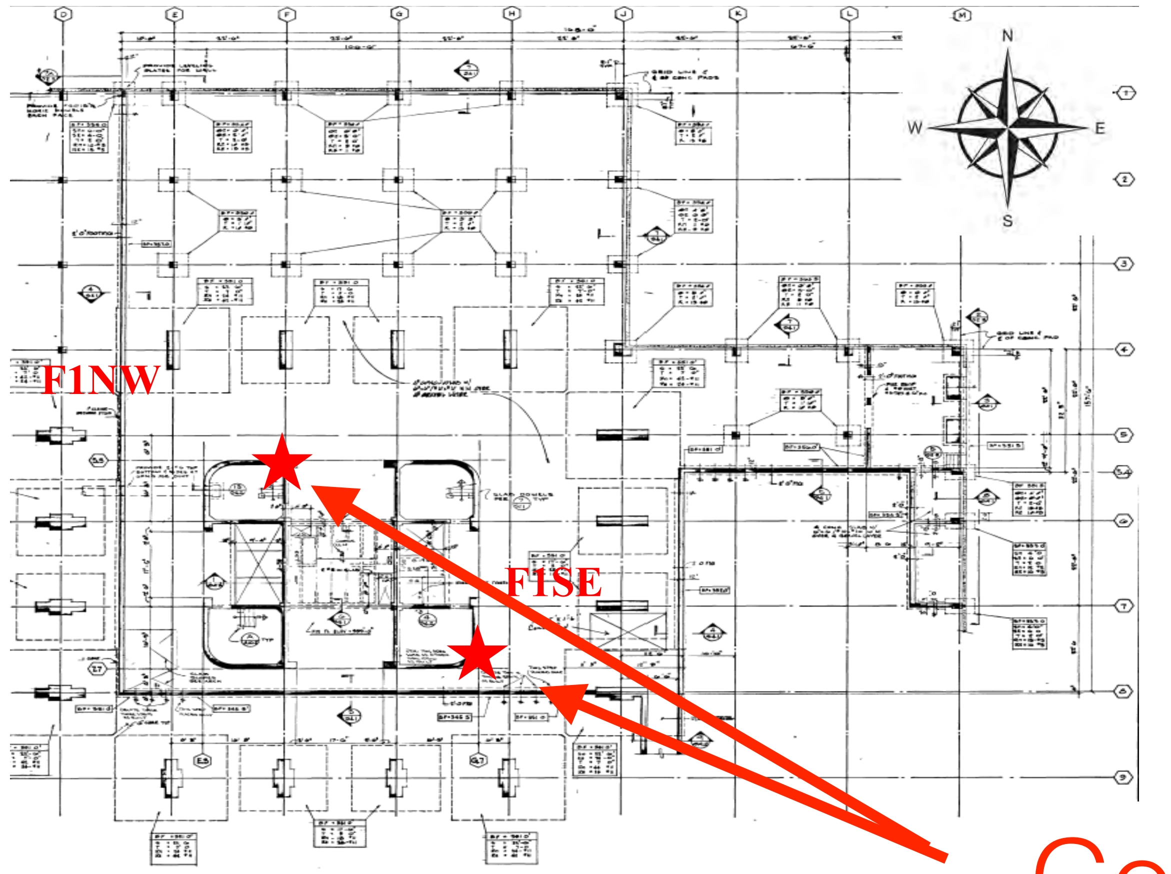

Fourth floor

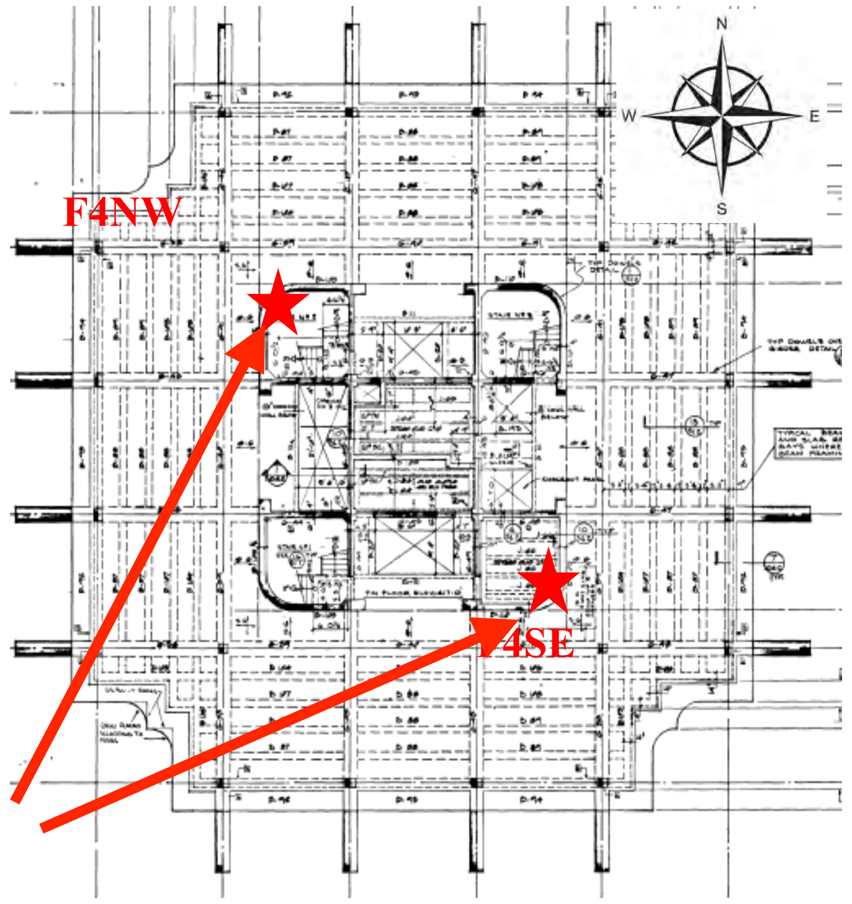

Sixth floor

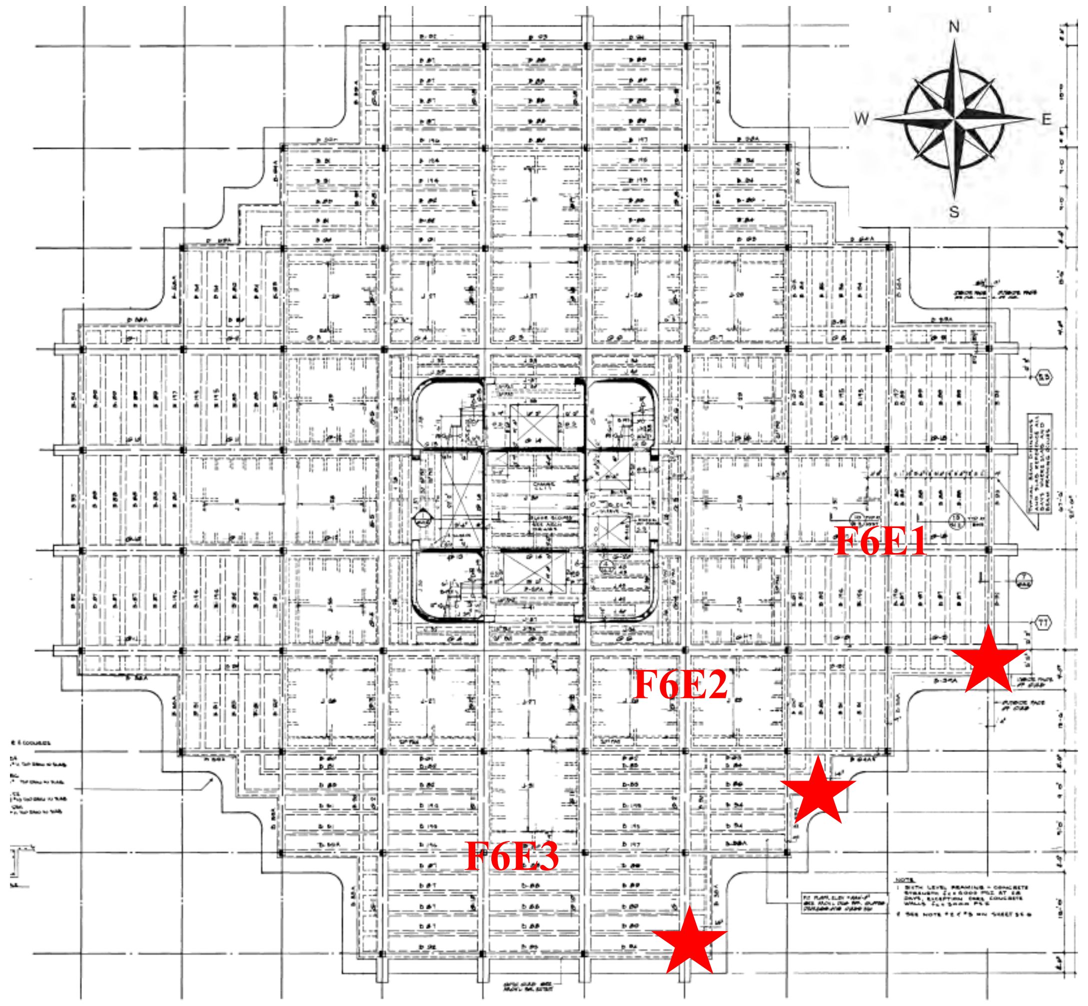

Seventh floor

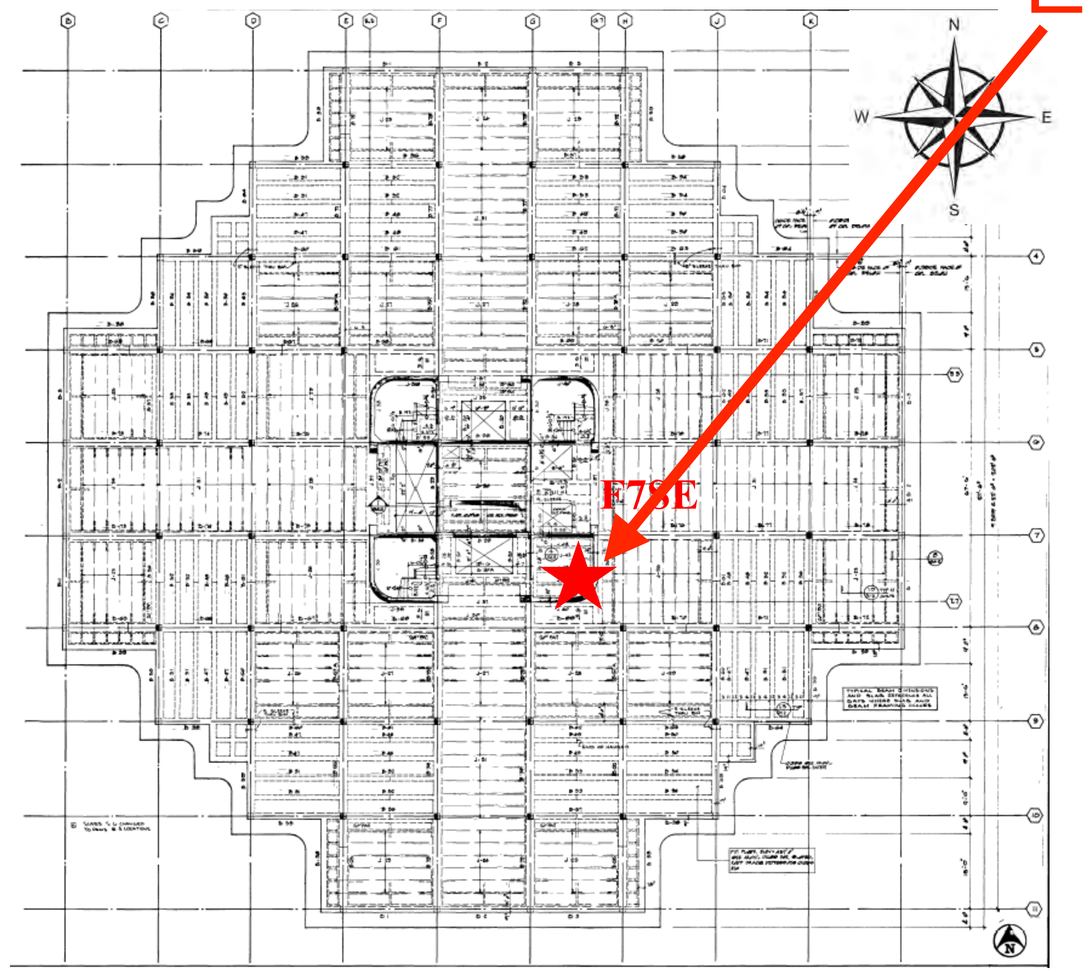

Core Wall Locations

Roof (Penthouse)

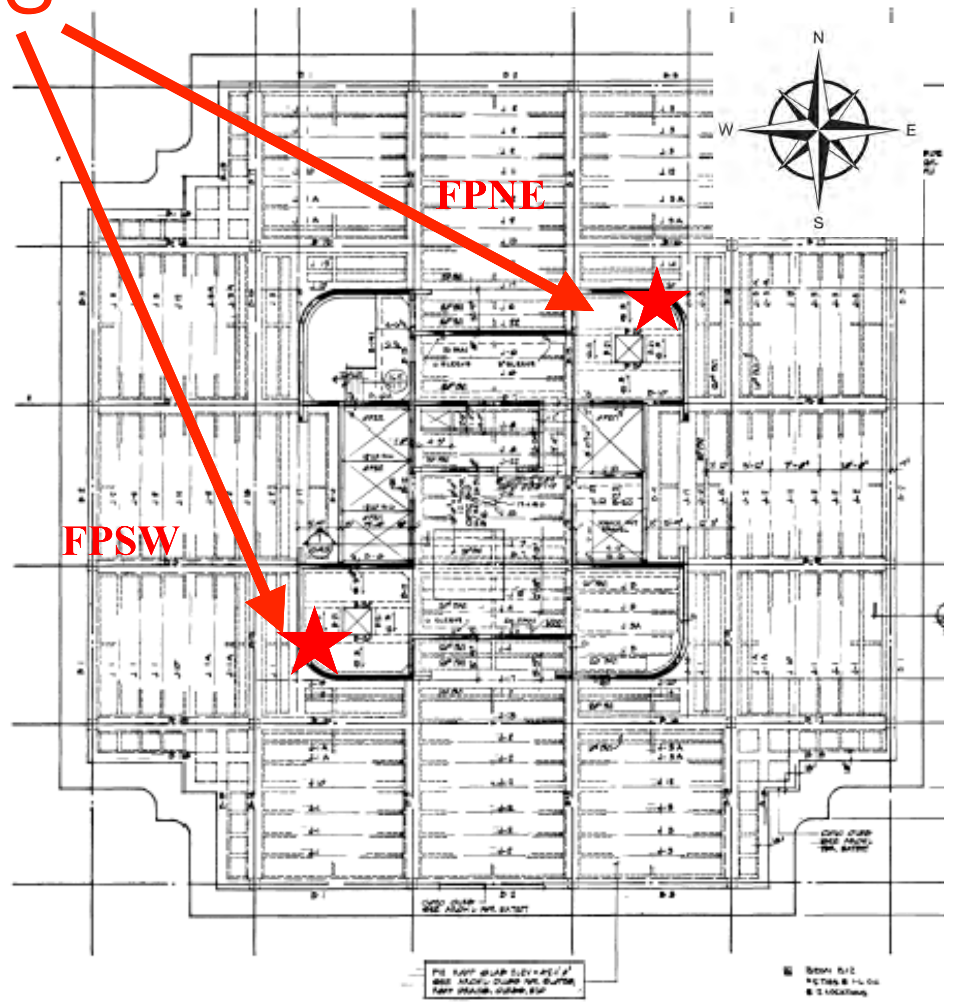

Locations of Accelerometers at Different Floors

Etna2 Accelerometer

First floor

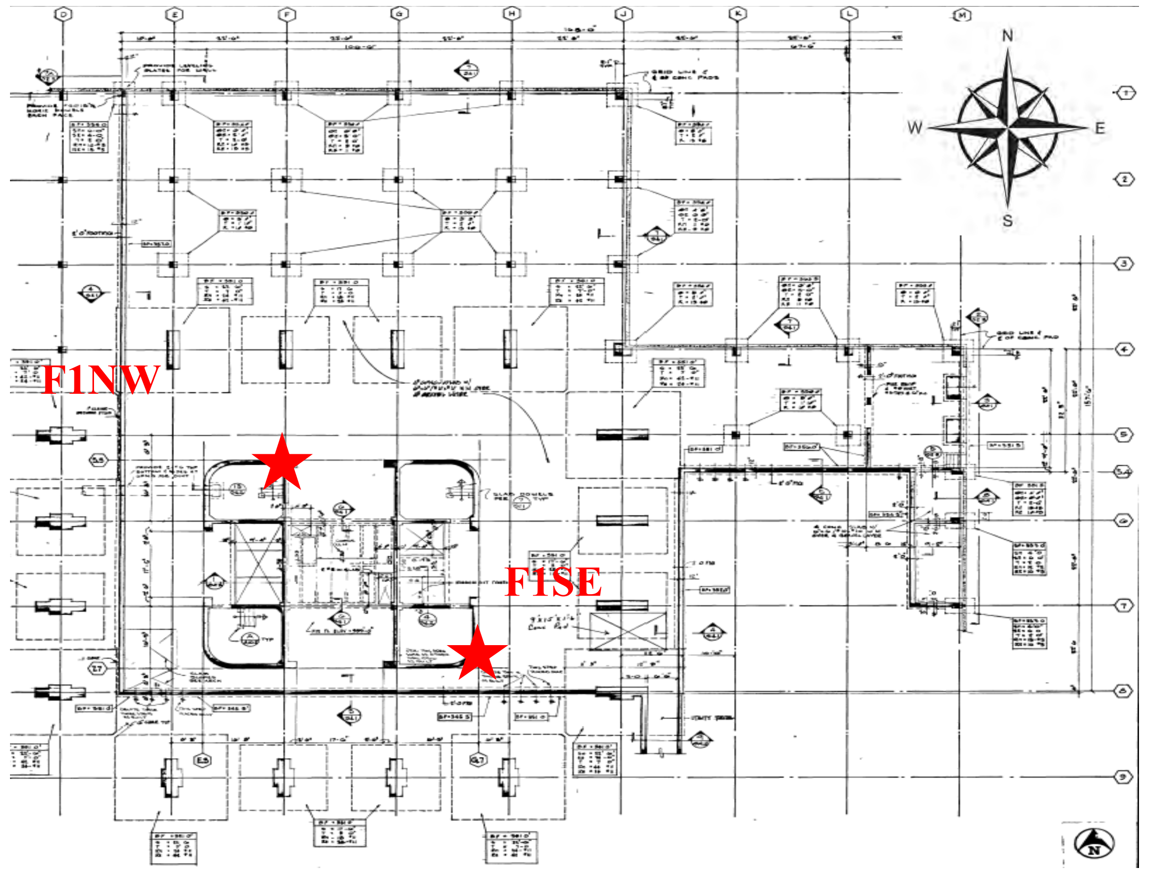

Fourth floor

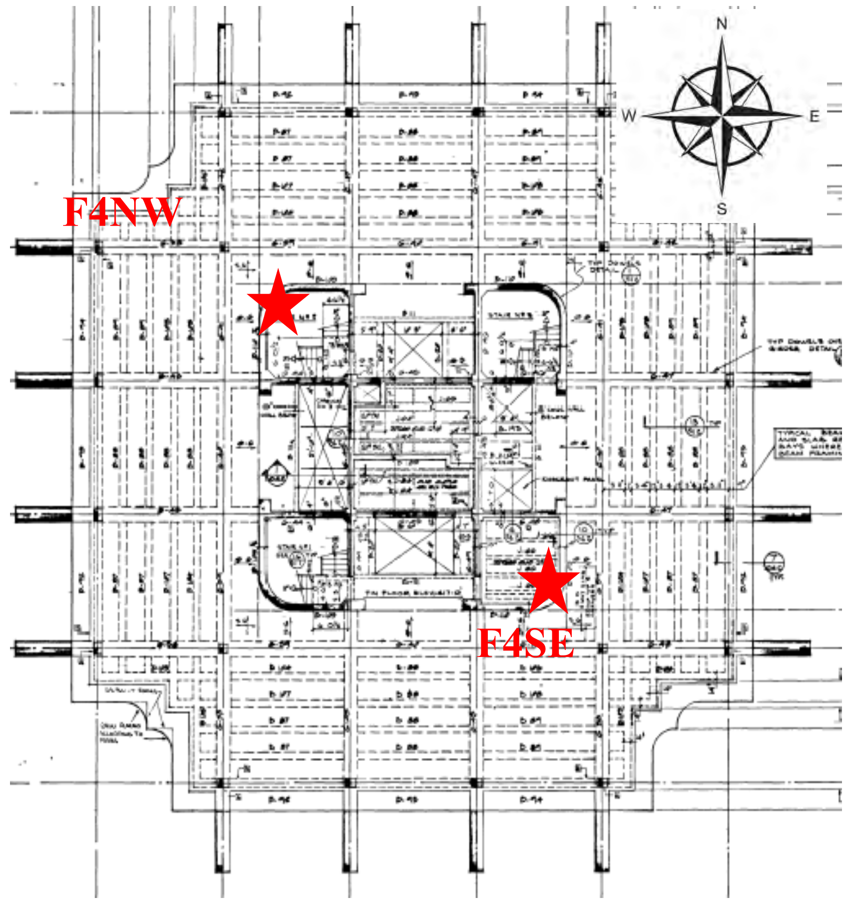

Sixth floor

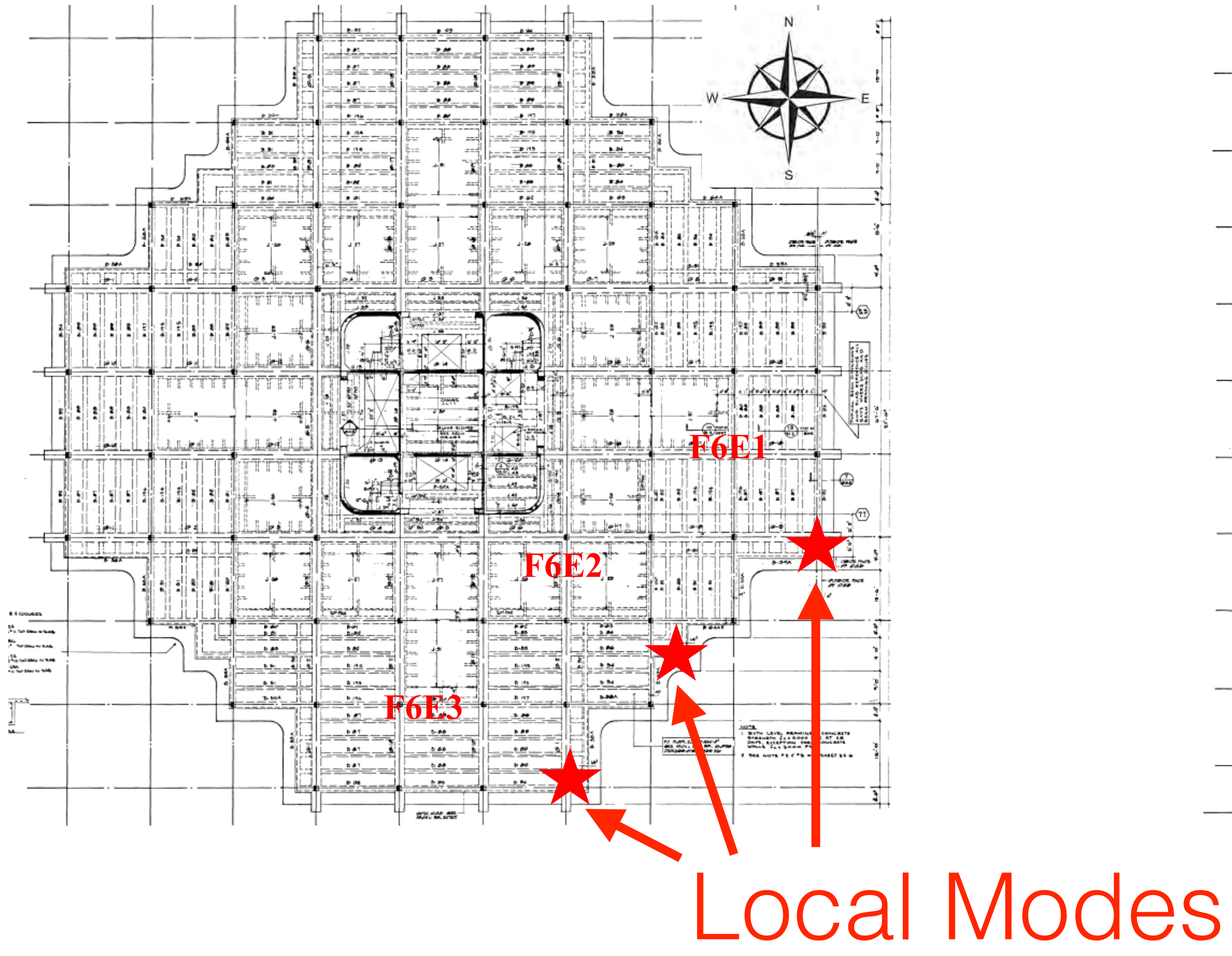

Seventh floor

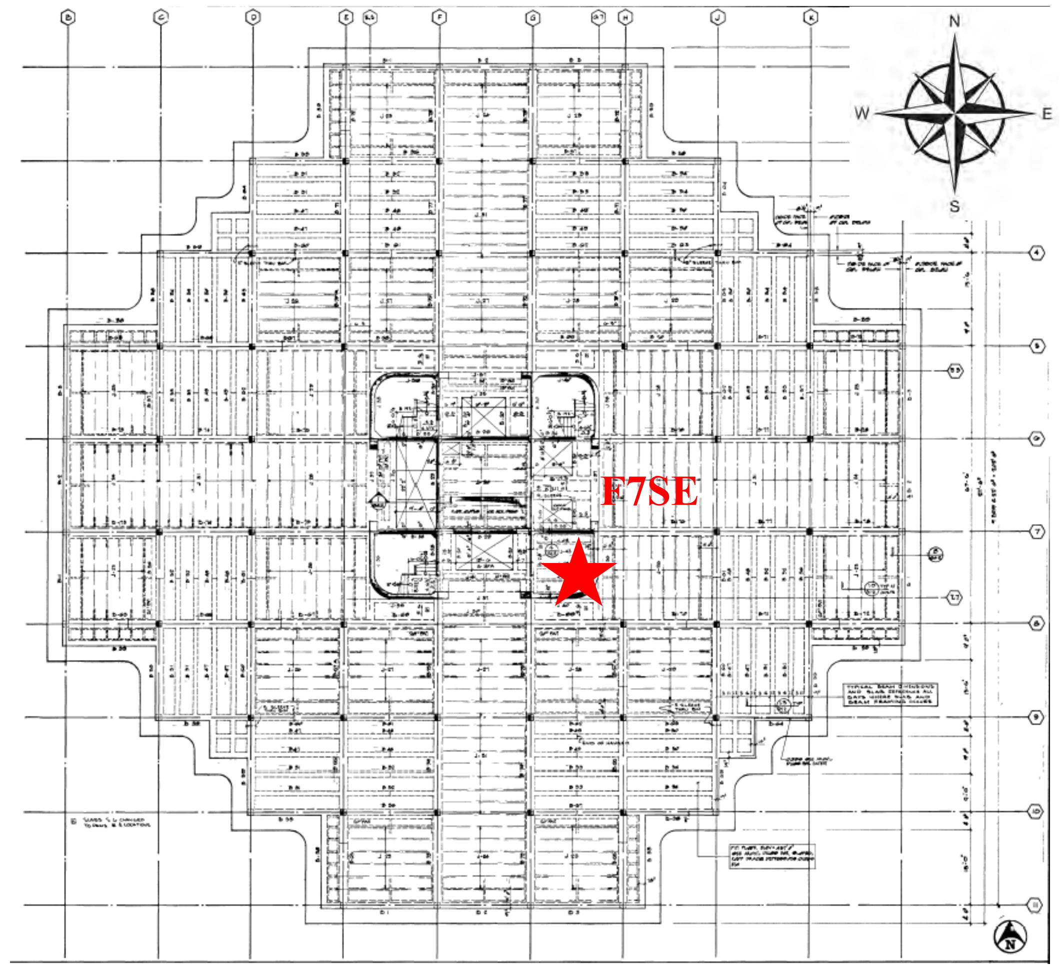

Roof (Penthouse)

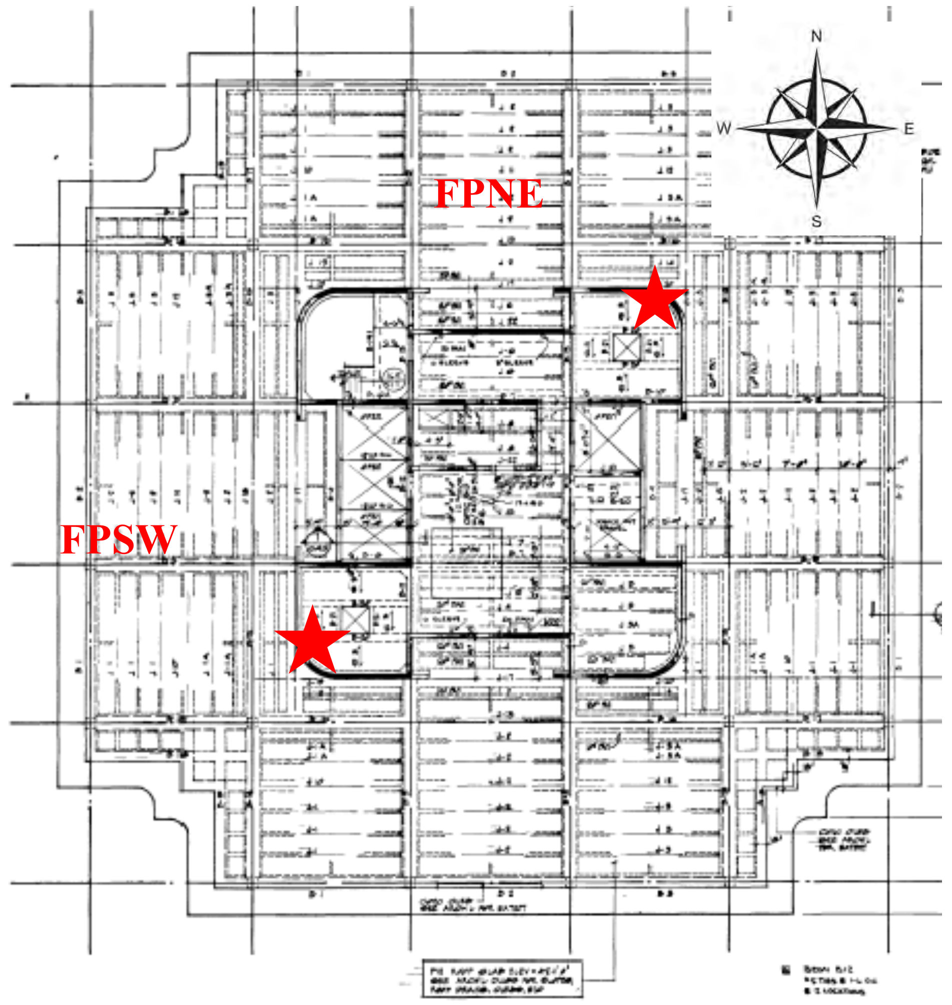

Observations

M 5.3 earthquake near Calipatria, CA
June 5th, 2021 17:55:58 (UTC)
33.140°   -115.635°
5.8 km depth

: UCSD Geisel Library

: Epicenter of earthquake

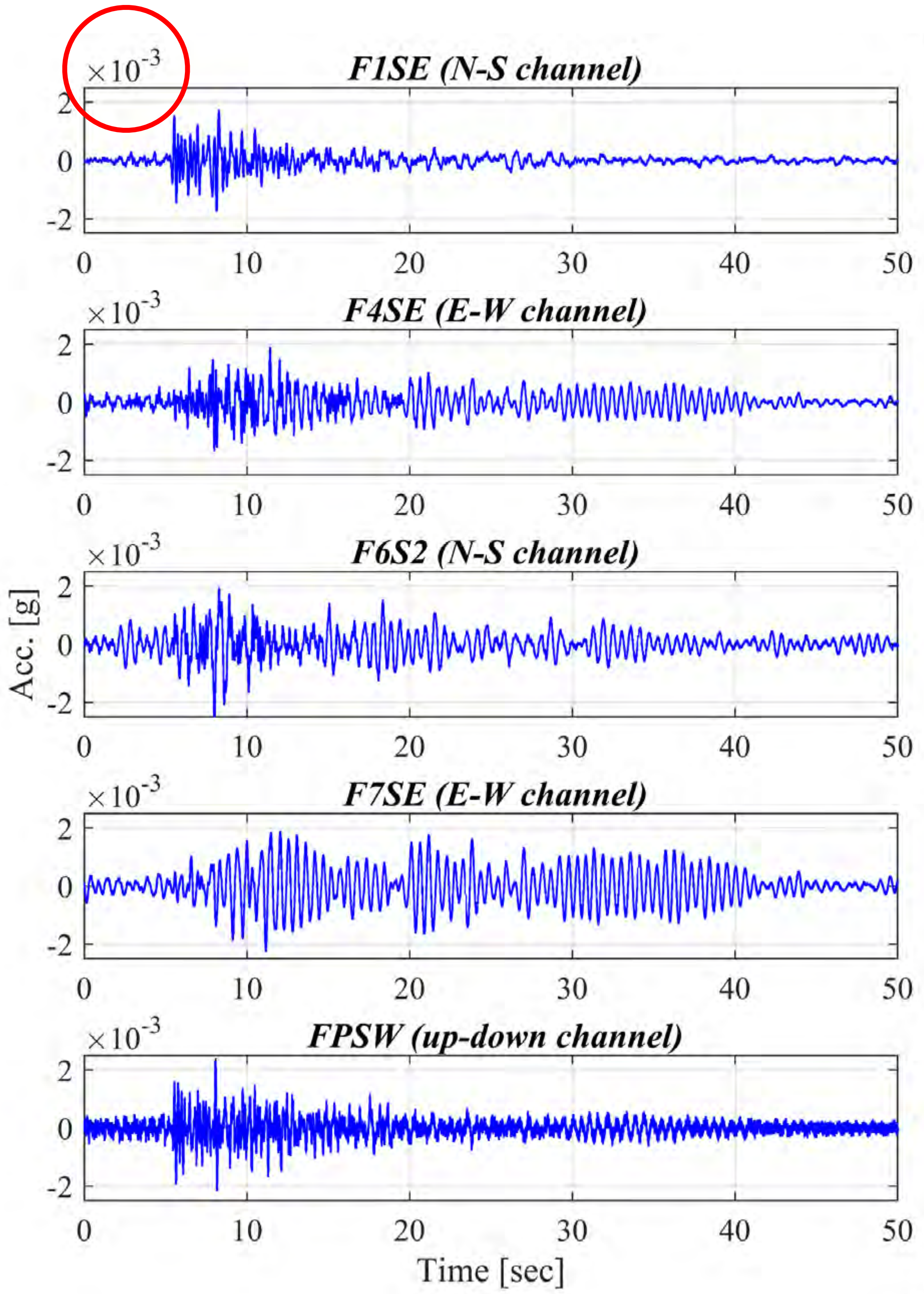

Recorded 08:00:00 to 08:00:30 UTC, September 11, 2021
Higher frequency content
Lower amplitude
than seismic data

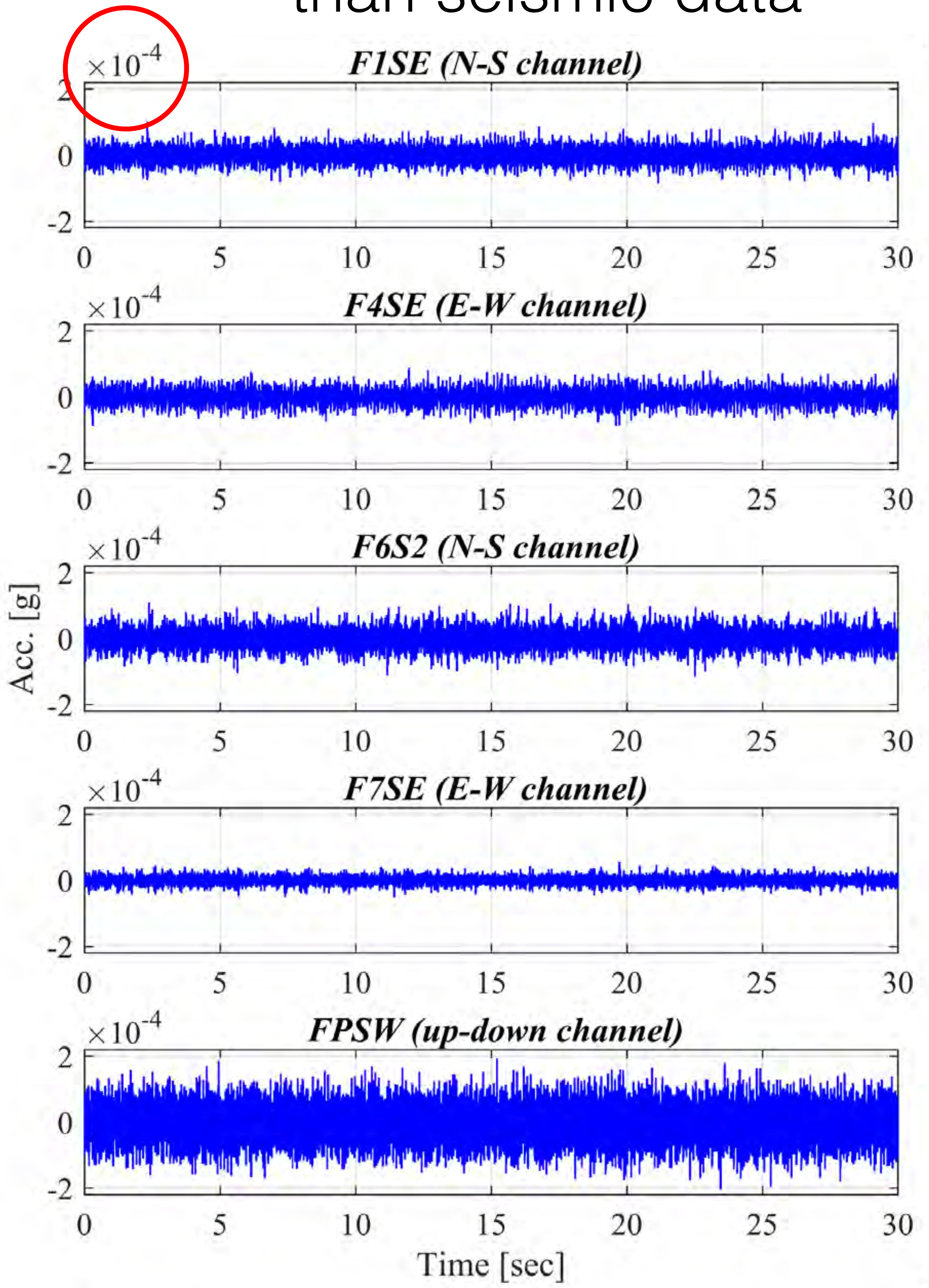

Observations

M 5.3 earthquake near Calipatria, CA
June 5th, 2021 17:55:58 (UTC)
33.140° -115.635°
5.8 km depth

★ : UCSD Geisel Library
★ : Epicenter of earthquake

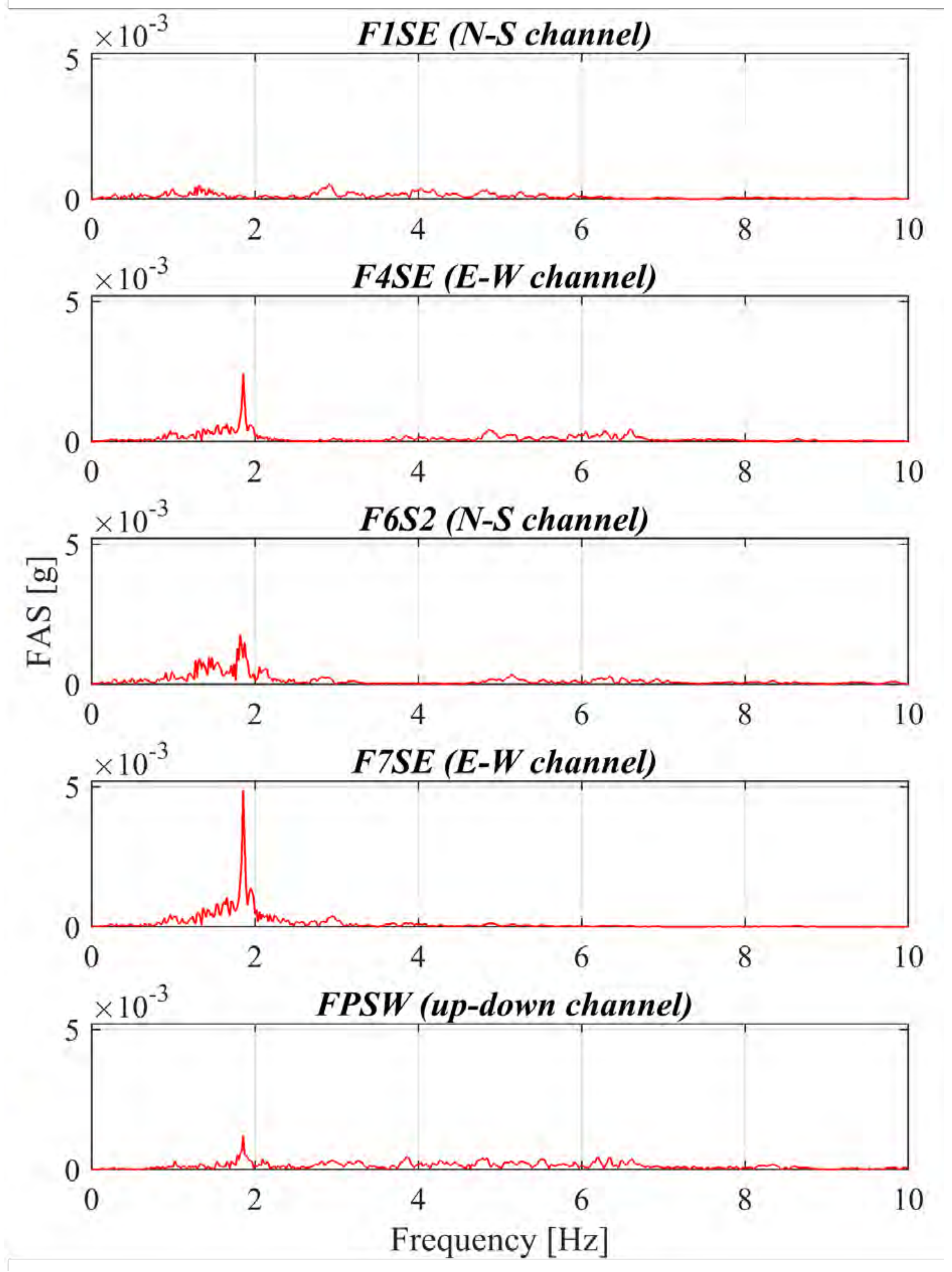

Recorded 08:00:00 to 08:00:30 UTC, September 11, 2021
Higher frequency content
Lower amplitude than seismic data

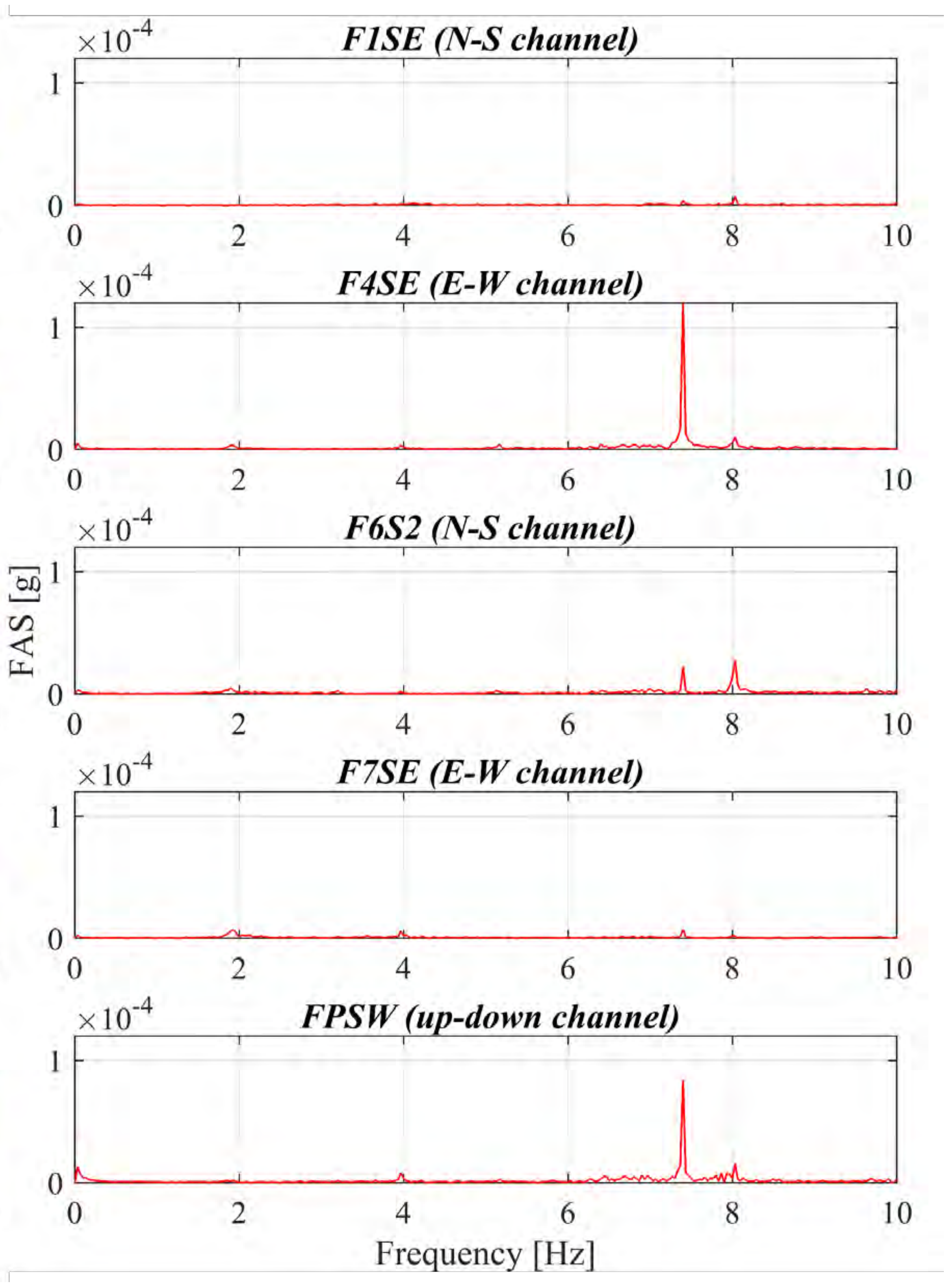

Environmental Observations Using Ambient Noise

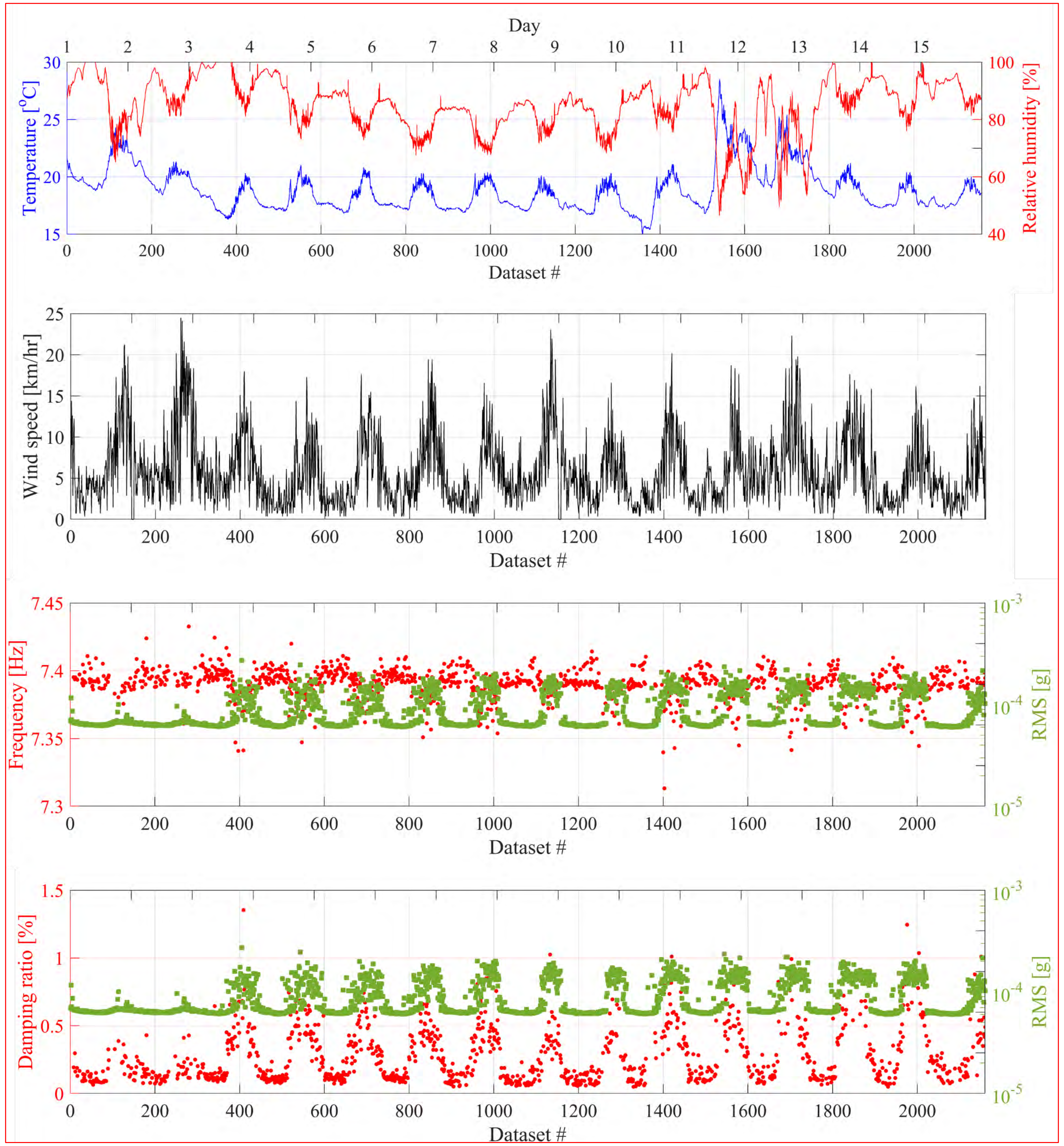

- 4th-TEW+To Mode
  - 7.39 Hz
  - 0.28 Damping Ratio
- Damping ratios show significantly higher variability than natural frequencies.
- Identified frequencies have negative correlation with temperature.
- Identified damping ratios have positive correlation with RMS roof acceleration.
- Relative effects of humidity, temperature, wind speed, RMS roof acceleration on identified modal properties cannot be discriminated.

Comparison between Modal Properties Identified Using Seismic data and Ambient Noise Data

Mode #	Abbreviation of mode
1	1st-To
2	1st-T^{NE-SW}
3	1st-T^{NW-SE}
4	2nd-T^{EW}+To
5	3rd-T^{EW}+To
6	1st-T^{EW}+To
7	4th-T^{EW}+To
8	5th-T^{EW}+To
9	6th-T^{EW}+To

Identified from seismic data (modes 1–6)

Identified from noise data (modes 6–9)

- Only one mode (1st-TEW+To) is identified from seismic data and from Ambient Noise data.
- Natural frequency of mode 1st-TEW-To identified by seismic data is 1.6% lower than that identified by Ambient Noise data.
- Damping ratio of mode 1st-TEW-To identified by seismic data is 7.1% higher than that identified by Ambient Noise data.

Linear Finite Element Model of the Geisel Library

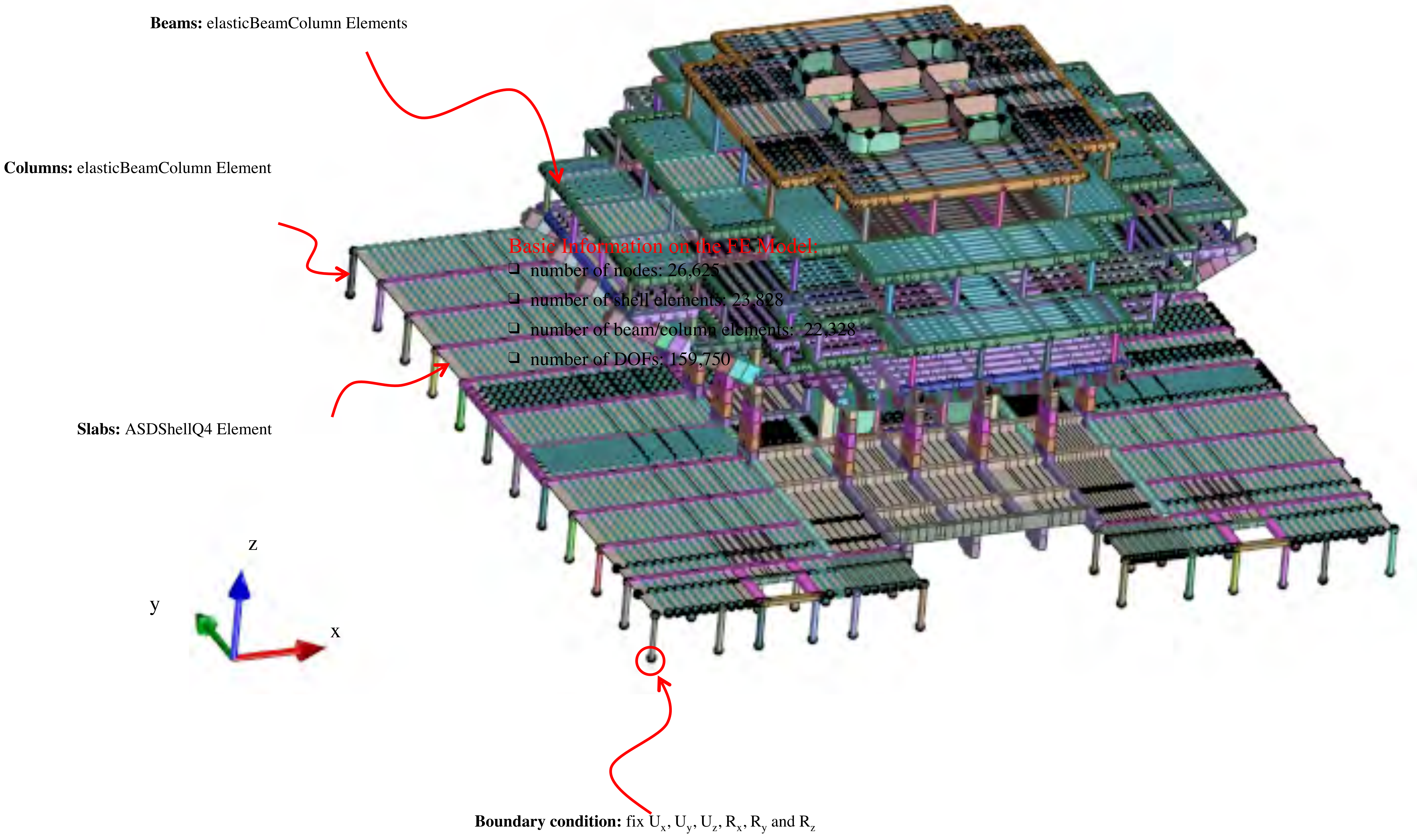

Finite Element Modeling Platform:

- FE analysis software framework OpenSees (the Open System for Earthquake Engineering Simulation)
- STKO (Scientific Toolkit for OpenSees)

Modeling Assumptions:

- linear elastic material behavior
- gross section properties are used
- soil-structure interaction effects are ignored

Basic Information on the FE Model:

- number of nodes: 26,625
- number of shell elements: 23,828
- number of beam/column elements: 22,328
- number of DOFs: 159,750

Finite Element Modeling of the Geisel Library

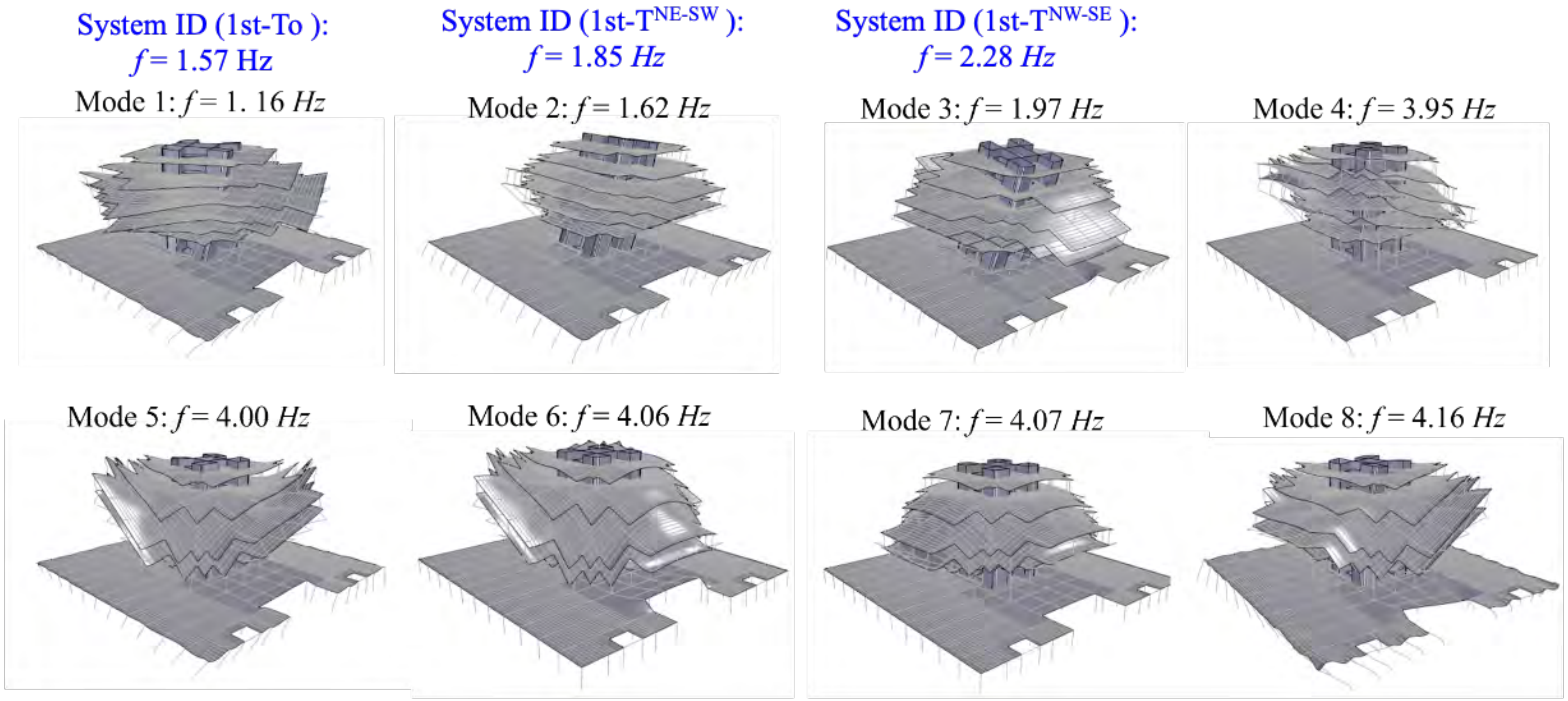

Sources of discrepancy between identified modes and computed modes:

- Mass associated to live load (books and bookshelves, students and library staff) is ignored in the FE model (increases the discrepancy)
- Actual current Youngs modulus of concrete is higher than the Young's modulus obtained from the specified compressive concrete strength of 4,350 psi (decreases the discrepancy)
- Cracking of concrete in the past 54 years is not accounted for (increases the discrepancy)

Results from Geisel Library

- Six vibration modes of the Geisel Library building were identified from the recorded seismic data using five Linear System ID methods
  - First six modes are global torsional and flexural modes or global coupled torsional-flexural modes.
  - The first four modes were identified as quasi-classically damped.
- Four modes were identified using the Stochastic Subspace Identification Data method and the ambient vibration datasets
  - These modes are higher modes than those identified using the seismic data.
  - Only one mode was identified from both sources of excitation.
  - The four modes identified from the ambient noise data are all global coupled torsional-flexural modes.
  - The identified damping ratios are much lower than those identified from the seismic data.
  - Strong correlations are observed between the time variations of the identified modal properties and the environmental conditions (wind speed, temperature, relative humidity).

UC San Diego NHERI Renewal Team

Joel Conte
PI, Site Admin.

John McCartney
Co-PI, Site User Services

Machel Morrison
Co-PI, Site Operations

José Restrepo
Co-PI, Site Performance

Lelli Van Den Einde
Co-PI, ECO

Tri-axial Strong Ground Motion Records Used to Design the 6-DOF Upgrade of the LHPOST

Event name	Station name	M	PGA (g)			PGV (m/s)			PGD (m)			High pass freq. (Hz)
			EW	NS	UP	EW	NS	UP	EW	NS	UP	
Tabas, 1978	Tabas, Iran	7.4	0.97	0.88	0.72	1.0	0.87	0.33	0.62	0.33	0.11	0.16
Chi-Chi, Taiwan, 1999	TCU065	7.6	0.72	0.49	0.23	0.82	0.73	0.38	0.36	0.24	0.10	0.25
Kobe, 1995	Takatori, Japan	6.9	0.62	0.67	0.28	1.21	1.23	0.16	0.40	0.30	0.04	0.125
Northridge, 1994	Rinaldi Receiving Station	6.7	0.87	0.47	0.96	1.48	0.75	0.42	0.42	0.23	0.04	0.10
Nepal, 2015	Kathmandu, Nepal	7.8	0.16	0.17	0.15	0.43	0.40	0.26	0.30	0.20	0.10	0.25
AC-156 compatible earthquake		–	1.01	0.96	0.71	1.04	1.13	0.77	0.22	0.21	0.12	0.70

Performance Characteristics of LHPOST6

Platen size	12.2 m × 7.6 m (40 ft × 25 ft)
Frequency Bandwidth	0–33 Hz
Vertical Payload Capacity	20 MN (4,500 kip)

	Sinusoidal motions—Bare table condition			Sinusoidal motions—Centered rigid payload of 4.9 MN (1,100 kips)		
	Horizontal X (E-W)	Horizontal Y (N-S)	Vertical Z (–)	Horizontal X (E-W)	Horizontal Y (N-S)	Vertical Z (–)
Peak Translational Displacement	±0.89 m (±35 in)	±0.38 m (±15 in)	±0.127 m (±5 in)	±0.89 m (±35 in)	±0.38 m (±15 in)	±0.127 m (±5 in)
Peak Translational Velocity	2.5 m/s (100 in/s)	2.0 m/s (80 in/s)	0.6 m/s (25 in/s)	2.5 m/s (100 in/s)	2.0 m/s (80 in/s)	0.6 m/s (25 in/s)
Peak Translational Acceleration	5.9 g	4.6 g	4.7 g (1)	1.6 g	1.2 g	2.0 g (1)
Peak Translational Force	10.6 MN (2,380 kip)	8.38 MN (1,890 kip)	54.8 MN (2) (12,300 kip)	10.6 MN (2,380 kip)	8.38 MN (1,890 kip)	54.8 MN (2) (12,300 kip)
Peak Rotation	2.22 deg (3)	1.45 deg (3)	4.0 deg	2.22 deg (3)	1.45 deg (3)	4.0 deg
Peak Rotational Velocity	21.0 deg/s	12.4 deg/s	40.5 deg/s	21.0 deg/s	12.4 deg/s	40.5 deg/s
Peak Moment	23.1 MN-m (17,000 kip-ft)	31.4 MN-m (23,200 kip-ft)	47.0 MN-m (34,600 kip-ft)	37.2 MN-m (27,400 kip-ft)	49.0 MN-m (36,200 kip-ft)	47.0 MN-m (34,600 kip-ft)
Overturning Moment Capacity	32.0 MN-m (23,600 kip-ft)	35.0 MN-m (25,800 kip-ft)		45.1 MN-m (33,200 kip-ft)	50.0 MN-m (36,900 kip-ft)	

Performance Characteristics of LHPOST6

Platen size	12.2 m × 7.6 m (40 ft × 25 ft)					
Frequency Bandwidth	0–33 Hz					
Vertical Payload Capacity	20 MN (4,500 kip)					
	Sinusoidal motions—Bare table condition			Sinusoidal motions—Centered rigid payload of 4.9 MN (1,100 kips)		
	Horizontal X (E-W)	Horizontal Y (N-S)	Vertical Z (–)	Horizontal X (E-W)	Horizontal Y (N-S)	Vertical Z (–)
Peak Translational Displacement	±0.89 m (±35 in)	±0.38 m (±15 in)	±0.127 m (±5 in)	±0.89 m (±35 in)	±0.38 m (±15 in)	±0.127 m (±5 in)
Peak Translational Velocity	2.5 m/s (100 in/s)	2.0 m/s (80 in/s)	0.6 m/s (25 in/s)	2.5 m/s (100 in/s)	2.0 m/s (80 in/s)	0.6 m/s (25 in/s)
Peak Translational Acceleration	5.9 g	4.6 g	4.7 g (1)	1.6 g	1.2 g	2.0 g (1)
Peak Translational Force	10.6 MN (2,380 kip)	8.38 MN (1,890 kip)	54.8 MN (2) (12,300 kip)	10.6 MN (2,380 kip)	8.38 MN (1,890 kip)	54.8 MN (2) (12,300 kip)
Peak Rotation	2.22 deg (3)	1.45 deg (3)	4.0 deg	2.22 deg (3)	1.45 deg (3)	4.0 deg
Peak Rotational Velocity	21.0 deg/s	12.4 deg/s	40.5 deg/s	21.0 deg/s	12.4 deg/s	40.5 deg/s
Peak Moment	23.1 MN-m (17,000 kip-ft)	31.4 MN-m (23,200 kip-ft)	47.0 MN-m (34,600 kip-ft)	37.2 MN-m (27,400 kip-ft)	49.0 MN-m (36,200 kip-ft)	47.0 MN-m (34,600 kip-ft)
Overturning Moment Capacity	32.0 MN-m (23,600 kip-ft)	35.0 MN-m (25,800 kip-ft)		45.1 MN-m (33,200 kip-ft)	50.0 MN-m (36,900 kip-ft)	

Performance Characteristics of LHPOST6

Platen size	12.2 m × 7.6 m (40 ft × 25 ft)
Frequency Bandwidth	0–33 Hz
Vertical Payload Capacity	20 MN (4,500 kip)

	Sinusoidal motions—Bare table condition			Sinusoidal motions—Centered rigid payload of 4.9 MN (1,100 kips)		
	Horizontal X (E-W)	Horizontal Y (N-S)	Vertical Z (–)	Horizontal X (E-W)	Horizontal Y (N-S)	Vertical Z (–)
Peak Translational Displacement	±0.89 m (±35 in)	±0.38 m (±15 in)	±0.127 m (±5 in)	±0.89 m (±35 in)	±0.38 m (±15 in)	±0.127 m (±5 in)
Peak Translational Velocity	2.5 m/s (100 in/s)	2.0 m/s (80 in/s)	0.6 m/s (25 in/s)	2.5 m/s (100 in/s)	2.0 m/s (80 in/s)	0.6 m/s (25 in/s)
Peak Translational Acceleration	5.9 g	4.6 g	4.7 g (1)	1.6 g	1.2 g	2.0 g (1)
Peak Translational Force	10.6 MN (2,380 kip)	8.38 MN (1,890 kip)	54.8 MN (2) (12,300 kip)	10.6 MN (2,380 kip)	8.38 MN (1,890 kip)	54.8 MN (2) (12,300 kip)
Peak Rotation	2.22 deg (3)	1.45 deg (3)	4.0 deg	2.22 deg (3)	1.45 deg (3)	4.0 deg
Peak Rotational Velocity	21.0 deg/s	12.4 deg/s	40.5 deg/s	21.0 deg/s	12.4 deg/s	40.5 deg/s
Peak Moment	23.1 MN-m (17,000 kip-ft)	31.4 MN-m (23,200 kip-ft)	47.0 MN-m (34,600 kip-ft)	37.2 MN-m (27,400 kip-ft)	49.0 MN-m (36,200 kip-ft)	47.0 MN-m (34,600 kip-ft)
Overturning Moment Capacity	32.0 MN-m (23,600 kip-ft)	35.0 MN-m (25,800 kip-ft)		45.1 MN-m (33,200 kip-ft)	50.0 MN-m (36,900 kip-ft)	

Performance Characteristics of LHPOST6

Platen size	12.2 m × 7.6 m (40 ft × 25 ft)
Frequency Bandwidth	0–33 Hz
Vertical Payload Capacity	20 MN (4,500 kip)

	Sinusoidal motions—Bare table condition			Sinusoidal motions—Centered rigid payload of 4.9 MN (1,100 kips)		
	Horizontal X (E-W)	Horizontal Y (N-S)	Vertical Z (–)	Horizontal X (E-W)	Horizontal Y (N-S)	Vertical Z (–)
Peak Translational Displacement	±0.89 m (±35 in)	±0.38 m (±15 in)	±0.127 m (±5 in)	±0.89 m (±35 in)	±0.38 m (±15 in)	±0.127 m (±5 in)
Peak Translational Velocity	2.5 m/s (100 in/s)	2.0 m/s (80 in/s)	0.6 m/s (25 in/s)	2.5 m/s (100 in/s)	2.0 m/s (80 in/s)	0.6 m/s (25 in/s)
Peak Translational Acceleration	5.9 g	4.6 g	4.7 g (1)	1.6 g	1.2 g	2.0 g (1)
Peak Translational Force	10.6 MN (2,380 kip)	8.38 MN (1,890 kip)	54.8 MN (2) (12,300 kip)	10.6 MN (2,380 kip)	8.38 MN (1,890 kip)	54.8 MN (2) (12,300 kip)
Peak Rotation	2.22 deg (3)	1.45 deg (3)	4.0 deg	2.22 deg (3)	1.45 deg (3)	4.0 deg
Peak Rotational Velocity	21.0 deg/s	12.4 deg/s	40.5 deg/s	21.0 deg/s	12.4 deg/s	40.5 deg/s
Peak Moment	23.1 MN-m (17,000 kip-ft)	31.4 MN-m (23,200 kip-ft)	47.0 MN-m (34,600 kip-ft)	37.2 MN-m (27,400 kip-ft)	49.0 MN-m (36,200 kip-ft)	47.0 MN-m (34,600 kip-ft)
Overturning Moment Capacity	32.0 MN-m (23,600 kip-ft)	35.0 MN-m (25,800 kip-ft)		45.1 MN-m (33,200 kip-ft)	50.0 MN-m (36,900 kip-ft)	

1978, M7.4 Tabas, Iran, Tri-Axial Ground Motion

Synthetic Six-Axial Ground Motion

1994 Northridge Earthquake (Rinaldi Station) – Tri-axial – 100%

Reconfigurable/Modular 3-D Full-Scale Three-Story Steel Testbed Building

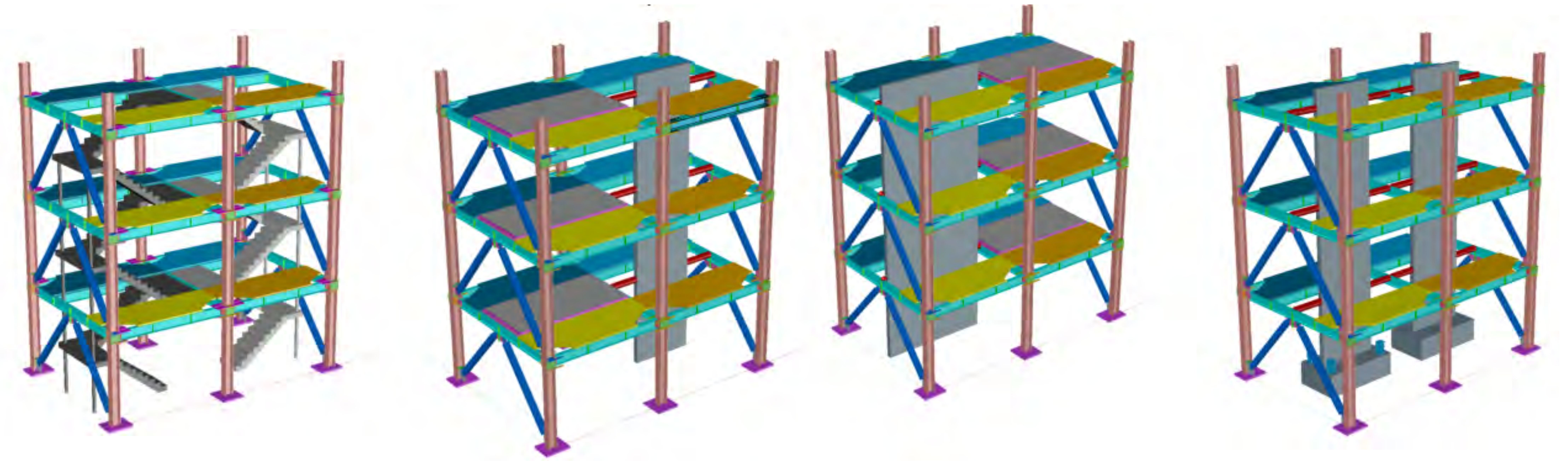

Modular Test Bed Building (MTB2) Project

Construction of NHERI TallWood Specimen

Construction of NHERI TallWood Specimen

Construction of NHERI TallWood Specimen

New Research Enabled by the LHPOST6

Investigate many important aspects of the seismic response behavior of civil infrastructure systems:

- **Effects of three-directional translational ground motions**
- **Effects of rotational ground motion components**
- **Effects of six-degree-of-freedom earthquake ground motions**

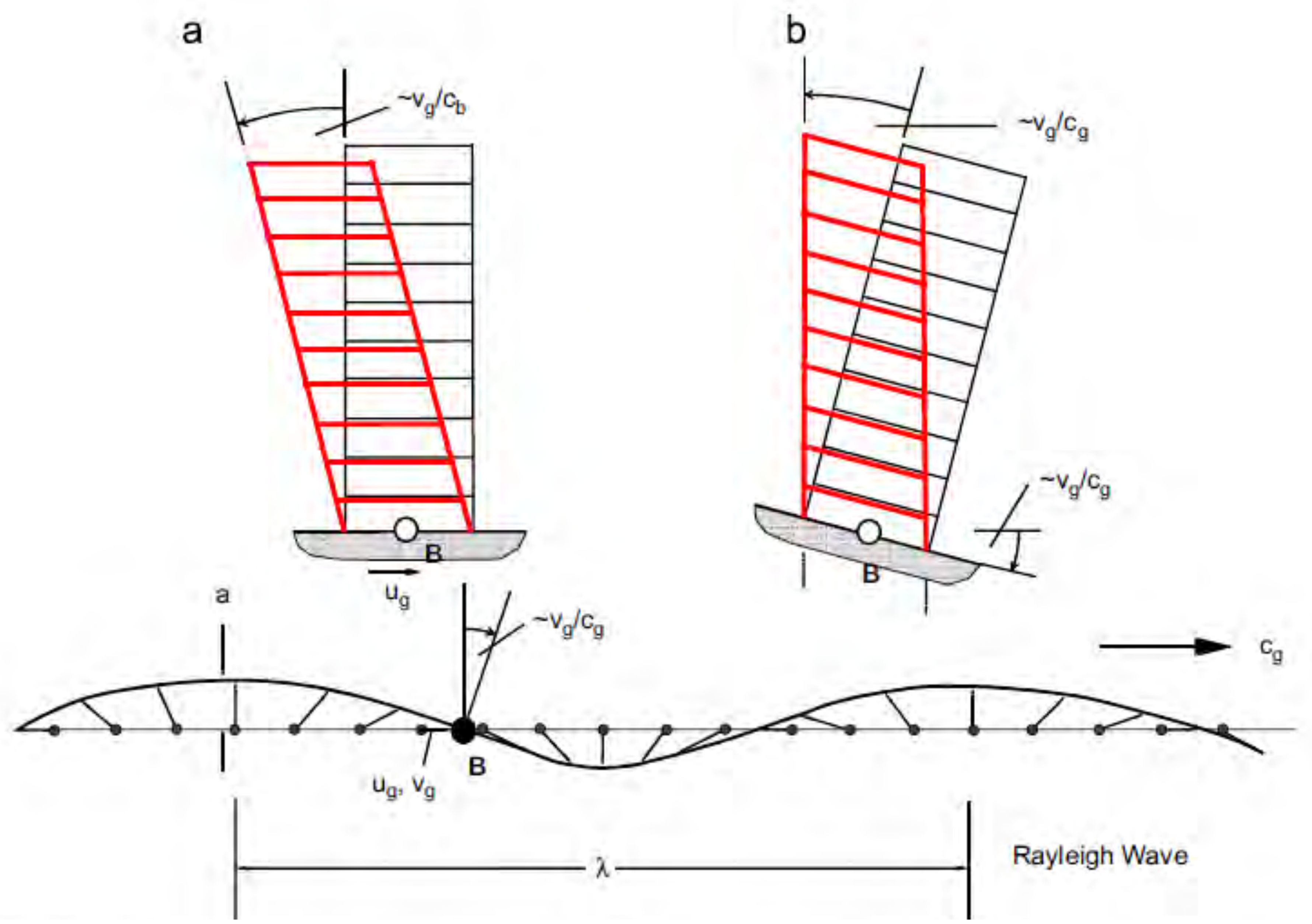

Geometric interpretation of how horizontal translation and rocking can contribute to the total drift in a simple building during passage of a Rayleigh wave [Trifunac, 2009]

For More Information About NHERI@UC San Diego Experimental Facility

- https://ucsd.designsafe-ci.org
- Contact one of the NHERI@UC San Diego team member:
  - Joel Conte, jpconte@ucsd.edu
  - John McCartney, mccartney@eng.ucsd.edu
  - Machel Morrison, mmorrison@eng.ucsd.edu
  - Jose Restrepo, jrestrepo@ucsd.edu
  - Lelli Van Den Einde, lellivde@ucsd.edu
  - Koorosh Lotfizadeh, klotfiza@ucsd.edu